THE EUROPEAN
PHYSICAL JOURNAL C

CrossMark

Measurement of the weak mixing angle using the forward–backward asymmetry of Drell–Yan events in pp collisions at 8 TeV

CMS Collaboration[*]

CERN, 1211 Geneva 23, Switzerland

Abstract A measurement is presented of the effective leptonic weak mixing angle ($\sin^2 \theta_{\text{eff}}^{\ell}$) using the forward–backward asymmetry of Drell–Yan lepton pairs ($\mu\mu$ and ee) produced in proton–proton collisions at $\sqrt{s} = 8$ TeV at the CMS experiment of the LHC. The data correspond to integrated luminosities of 18.8 and 19.6 fb^{-1} in the dimuon and dielectron channels, respectively, containing 8.2 million dimuon and 4.9 million dielectron events. With more events and new analysis techniques, including constraints obtained on the parton distribution functions from the measured forward–backward asymmetry, the statistical and systematic uncertainties are significantly reduced relative to previous CMS measurements. The extracted value of $\sin^2 \theta_{\text{eff}}^{\ell}$ from the combined dilepton data is $\sin^2 \theta_{\text{eff}}^{\ell} = 0.23101 \pm 0.00036\,(\text{stat}) \pm 0.00018\,(\text{syst}) \pm 0.00016\,(\text{theo}) \pm 0.00031\,(\text{parton distributions in proton}) = 0.23101 \pm 0.00053$.

1 Introduction

We report a measurement of the effective leptonic weak mixing angle ($\sin^2 \theta_{\text{eff}}^{\ell}$) using the forward–backward asymmetry (A_{FB}) in Drell–Yan $q\bar{q} \to \ell^+\ell^-$ events, where ℓ stands for muon (μ) or electron (e). The analysis is based on data from the CMS experiment at the CERN LHC. At leading order (LO), lepton pairs are produced through the annihilation of a quark with its antiquark into a Z boson or a virtual photon: $q\bar{q} \to Z/\gamma \to \ell^+\ell^-$. For a given dilepton invariant mass $m_{\ell\ell}$, the differential cross section at LO can be expressed at the parton level as

$$\frac{d\sigma}{d(\cos\theta^*)} \propto 1 + \cos^2\theta^* + A_4 \cos\theta^*, \tag{1}$$

where the $(1 + \cos^2\theta^*)$ term arises from the spin-1 of the exchanged boson, and the $\cos\theta^*$ term originates from inter-

ference between vector and axial-vector contributions. The definition of A_{FB} is based on the angle θ^* of the negative lepton (ℓ^-) in the Collins–Soper [1] frame of the dilepton system:

$$A_{\text{FB}} = \frac{3}{8} A_4 = \frac{\sigma_{\text{F}} - \sigma_{\text{B}}}{\sigma_{\text{F}} + \sigma_{\text{B}}}, \tag{2}$$

where σ_{F} and σ_{B} are, respectively, the cross sections in the forward ($\cos\theta^* > 0$) and backward ($\cos\theta^* < 0$) hemispheres. In this frame, θ^* is the angle of the ℓ^- relative to the axis that bisects the angle between the direction of the quark and the reversed direction of the antiquark. In proton–proton (pp) collisions, the direction of the quark is more likely to be in the direction of the Lorentz boost of the dilepton. Therefore, $\cos\theta^*$ can be calculated using the following variables in the laboratory frame:

$$\cos\theta^* = \frac{2(P_1^+ P_2^- - P_1^- P_2^+)}{\sqrt{m_{\ell\ell}^2(m_{\ell\ell}^2 + p_{\text{T},\ell\ell}^2)}} \frac{p_{z,\ell\ell}}{|p_{z,\ell\ell}|}, \tag{3}$$

where $m_{\ell\ell}$, $p_{\text{T},\ell\ell}$, and $p_{z,\ell\ell}$ are the mass, transverse momentum, and longitudinal momentum, respectively, of the dilepton system, and the $P_i^{\pm}$ are defined in terms of the energies (E_i) and longitudinal momenta ($p_{z,i}$), of the negatively and positively charged leptons as $P_i^{\pm} = (E_i \pm p_{z,i})/\sqrt{2}$ [1].

A non-zero A_{FB} value in dilepton events arises from the vector and axial-vector couplings of electroweak bosons to fermions. At LO, these respective couplings of Z bosons to fermions (f) can be expressed as:

$$v_{\text{f}} = T_3^{\text{f}} - 2Q_{\text{f}} \sin^2\theta_{\text{W}}, \tag{4}$$
$$a_{\text{f}} = T_3^{\text{f}}, \tag{5}$$

where Q_{f} and T_3^{f} are the charge and the third component of the weak isospin of the fermion, respectively, and $\sin^2\theta_{\text{W}}$ refers to the weak mixing angle, which is related to the masses
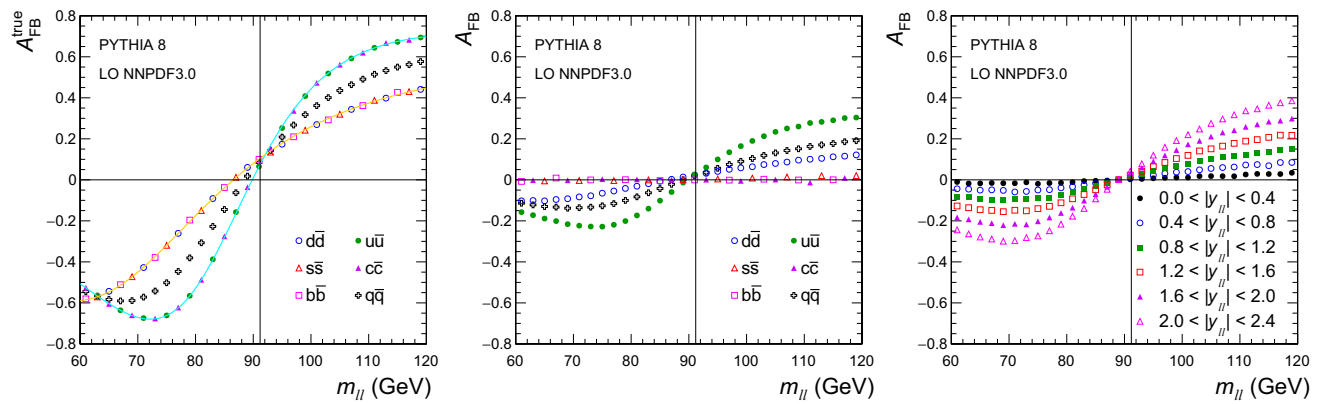
Springer

Fig. 1 The dependence of A_{FB} on $m_{\ell\ell}$ in dimuon events generated using PYTHIA 8.212 [16] and the LO NNPDF3.0 [17] PDFs for dimuon rapidities of $|y_{\ell\ell}| < 2.4$. The distributions for the total production ($q\bar{q}$) and the different channels are given on the left, overlaid with results based on Eq. (6), using the definition of $A_{FB}^{true}(m_{\ell\ell})$ for the known quark direction. The middle panel gives the diluted A_{FB} using instead the direction of the dilepton boost, and the right panel shows the diluted A_{FB} in $|y_{\ell\ell}|$ bins of 0.4 for all channels

of the W and Z bosons through the relation $\sin^2 \theta_W = 1 - m_W^2/m_Z^2$. Electroweak (EW) radiative corrections affect these LO relations. In the improved Born approximation [2,3], some of the higher-order corrections are absorbed into an effective mixing angle. The effective weak mixing angle is based on the relation $v_f/a_f = 1 - 4|Q_f| \sin^2 \theta_{eff}^f$, with $\sin^2 \theta_{eff}^f = \kappa_f \sin^2 \theta_W$, where the flavor-dependent κ_f is determined through EW corrections. The A_{FB} for dilepton events is sensitive primarily to $\sin^2 \theta_{eff}^\ell$.

We measure $\sin^2 \theta_{eff}^\ell$ by fitting the mass and rapidity ($y_{\ell\ell}$) dependence of the observed A_{FB} in dilepton events to standard model (SM) predictions as a function of $\sin^2 \theta_{eff}^\ell$. The most precise previous measurements of $\sin^2 \theta_{eff}^\ell$ were performed by the combined LEP and SLD experiments [4]. There is, however, a known discrepancy of about 3 standard deviations between the two most precise values. Other measurements of $\sin^2 \theta_{eff}^\ell$ have also been reported by the Tevatron and LHC experiments [5–15].

Using the LO expressions for the Z boson, virtual photon exchange, and their interference, the "true" A_{FB} (i.e., using the quark direction in the definition of $\cos \theta^*$) can be evaluated as

$$
\begin{aligned}
A_{FB}^{true}(m_{\ell\ell}) = {} & a_\ell a_q (8 v_\ell v_q - Q_q K D_m) \\
& \times [16(v_\ell^2 + a_\ell^2)(v_q^2 + a_q^2) - 8 v_\ell v_q Q_q K D_m \\
& + Q_q^2 K^2 (D_m^2 + \Gamma_Z^2/m_Z^2)]^{-1},
\end{aligned} \tag{6}
$$

where the subscript q refers to the participating quark, $K = 8\sqrt{2}\pi\alpha/G_F m_Z^2$, $D_m = 1 - m_Z^2/m_{\ell\ell}^2$, α is the electromagnetic coupling, G_F is the Fermi constant, and Γ_Z is the full decay width of the Z boson. A strong dependence of A_{FB} on $m_{\ell\ell}$ originates from axial and vector interference. The A_{FB} is negative at small $m_{\ell\ell}$ and positive at large values, crossing $A_{FB} = 0$ slightly below the Z boson peak.

In collisions of hadrons, A_{FB} is sensitive to parton distribution functions (PDFs) for two reasons. First, the different couplings of u- and d-type quarks to EW bosons generate different A_{FB} values in the corresponding production channels, which means that the average depends on the relative contributions of u- and d-type quarks to the total cross section. Second, the definition of A_{FB} in pp collisions is based on the sign of $y_{\ell\ell}$, which relies on the fact that on average the dilepton pairs are Lorentz-boosted in the quark direction. Therefore, a non-zero average A_{FB} originates only from valence-quark production channels and is diluted by events where the antiquark carries a larger momentum than the quark. A dependence of the "true" and diluted A_{FB} on dilepton mass for different $q\bar{q}$ production channels and their sum is shown in Fig. 1.

The dilution of A_{FB} depends strongly on $y_{\ell\ell}$, as shown in Fig. 1. At zero rapidity, the quark and antiquark carry equal momenta, and the dilution is maximal, resulting in $A_{FB} = 0$. The A_{FB} is measured in 12 bins of dilepton mass, covering the range $60 < m_{\ell\ell} < 120$ GeV, and 6 $|y_{\ell\ell}|$ bins of equal size for $|y_{\ell\ell}| < 2.4$. The boundaries in the dilepton mass are at: 60, 70, 78, 84, 87, 89, 91, 93, 95, 98, 104, 112, and 120 GeV. The mass bins are chosen such that near m_Z the bin widths are larger than the mass resolution in any of the ranges of $y_{\ell\ell}$. Smaller and larger mass bins are chosen such that all mass bins contain enough events to perform a meaningful independent measurement. The weak dependence of A_{FB} on $p_{T,\ell\ell}$ is included in the SM predictions. The uncertainty originating from modeling of $p_{T,\ell\ell}$ is very small and included in the theoretical estimates.

2 The CMS detector

The central feature of the CMS apparatus is a superconducting solenoid of 6 m internal diameter, providing a magnetic field of 3.8 T. A silicon pixel and strip tracker, a lead tungstate crystal electromagnetic calorimeter (ECAL), and a brass and

scintillator hadron calorimeter (HCAL), each composed of a barrel and two endcap sections reside within the solenoid volume. Forward calorimeters extend the pseudorapidity η coverage provided by the barrel and endcap detectors. Muons are measured in gas-ionization detectors embedded in the steel flux-return yoke outside the solenoid. A more detailed description of the CMS detector can be found in Ref. [18].

Muons are measured in the range $|\eta| < 2.4$, using detection planes based on the drift-tube, cathode-strip chamber, or resistive-plate chamber technologies. Matching muons to tracks measured in the silicon tracker provides a relative transverse momentum resolution for muons with $20 < p_T < 100$ GeV of 1.3–2.0% in the barrel, and less than 6% in the endcaps. The p_T resolution in the barrel is smaller than 10% for muons with p_T up to 1 TeV [19].

The electromagnetic calorimeter consists of 75 848 lead tungstate crystals that provide a coverage of $|\eta| < 1.48$ in the barrel region and $1.48 < |\eta| < 3.00$ in the two endcap regions. Preshower detectors consisting of two planes of silicon sensors, interleaved with a total of 3 radiation lengths of lead, are located in front of each endcap detector. The electron momentum is obtained by combining the energy measurement in the ECAL with that in the tracker. The momentum resolution for electrons with $p_T \approx 45$ GeV from Z $\rightarrow$ ee decays, ranges from 1.7% for nonshowering electrons in the barrel region, to 4.5% for showering electrons in the endcaps [20].

Events of interest are selected using a two-tiered trigger system [21]. The first level, consisting of custom hardware processors, uses information from the calorimeters and muon detectors to select events at a rate of about 100 kHz within a time interval of less than 4 μs. The second level, known as the high-level trigger, consists of a farm of processors running a version of the full event reconstruction software optimized for fast processing, that reduces the event rate to about 1 kHz before data storage.

3 Data and simulated events

The measurement is based on pp collisions at $\sqrt{s} = 8$ TeV recorded by the CMS Experiment in 2012, corresponding to integrated luminosities of 18.8 and 19.6 fb^{-1} for muon and electron channels, respectively.

Candidates for the dimuon channel are collected using an isolated single-muon trigger with a p_T threshold of 24 GeV and $|\eta| < 2.4$. At the beginning of data taking, the muon trigger was restricted to $|\eta| < 2.1$. We do not use these events, and the integrated luminosity in the dimuon analysis is therefore somewhat smaller than for dielectrons. Background contamination is reduced by applying identification and isolation criteria to the reconstructed muons. First, muon tracks are required to be reconstructed independently in the

inner tracker and in the outer muon detectors. A global fit to the momentum, including both tracker and muon detector hits, must have a fitted $\chi^2/$dof < 10, where dof stands for the degrees of freedom. Muon tracks are required to pass within a transverse distance of 0.2 cm from the primary vertex, defined as the pp vertex with the largest $\sum p_T^2$ of its associated tracks. Muon candidates are rejected if the scalar-p_T sum of all tracks within a cone of $\Delta R = \sqrt{(\Delta\eta)^2 + (\Delta\phi)^2} = 0.3$ around the muon is larger than 10% of the p_T of the muon (this is referred to as track isolation, with ϕ being the azimuth in radians). The track isolation requirement is insensitive to contributions from additional soft pp interactions (pileup). An event is selected when there are at least two isolated muons, with the leading muon (i.e., the one with largest p_T) having $p_T > 25$ GeV, and the next-to-leading muon having $p_T > 15$ GeV. At least one muon with $p_T > 25$ GeV is required to trigger the event. For the Drell–Yan signal, the two leptons are required to have opposite sign (OS).

Dielectron candidates are collected using a single-electron trigger with a p_T threshold of 27 GeV and $|\eta| < 2.5$. Variables pertaining to the energy distribution in electromagnetic showers and to impact parameters of inner tracks are used to separate prompt electrons from electrons originating from photon conversions in detector material. The jet background from SM events produced through quantum chromodynamics (QCD) is referred to as multijet production. A particle-flow (PF) event reconstruction algorithm is used to identify different particle types (photons, electrons, muons, and charged and neutral hadrons [22]). The scalar-p_T sum of all PF particles in a cone of $\Delta R < 0.3$ around the electron direction is required to be less than 15% of the electron p_T, which reduces the background from hadrons in multijet events that are reconstructed incorrectly as electrons. This sum is corrected for contributions from pileup [20]. The electron momentum is evaluated by combining the energy in the ECAL with the momentum in the tracker. To ensure good reconstruction, the coverage is restricted to $|\eta| < 2.4$, excluding the transition region of $1.44 < |\eta| < 1.57$ between the ECAL barrel and endcap detectors, as electron reconstruction in this region is not optimal. Dielectron candidates are selected when at least two OS electrons pass all quality requirements. The leading and next-to-leading electrons must have respectively $p_T > 30$ and > 20 GeV, with the triggering electron always required to have $p_T > 30$ GeV.

A total of about 8.2 million dimuon and 4.9 million dielectron candidate events are selected for further analysis. The number of dielectron events is smaller because of the higher p_T thresholds and more stringent selection criteria implemented in electron selections. The $Z/\gamma \rightarrow \mu^+\mu^-$ and $Z/\gamma \rightarrow e^+e^-$ data include small ($<$1%) background contaminations that originate from $Z/\gamma \rightarrow \tau^+\tau^-$, $t\bar{t}$, single top quark, and diboson (WW, WZ, and ZZ) events, as well as multijet and W+jets events. Contributions from these

backgrounds are subtracted from data as described below. Contamination from photon-induced background near the Z boson peak is negligible [23].

Monte Carlo (MC) simulation is used to model signal and background processes. The signal as well as the single-boson and top quark backgrounds are based on next-to-leading order (NLO) matrix elements implemented in the POWHEG v1 event generator [24–27] using the CT10 [28] PDFs. The generator is interfaced to PYTHIA 6.426 [29] using the Z2* [30,31] underlying event tune, which generates the parton showering, the hadronization, and the electromagnetic final-state radiation (FSR). The background events from τ lepton decays are simulated with TAUOLA 2.7 [32]. Diboson and multijet background events are generated with PYTHIA 6 using the CTEQ6L1 PDFs [33]. Simulated minimum-bias events are superimposed on the hard-interaction events to model the effects from pileup. The detector response to all particles is simulated through GEANT4 [34], and all final-state objects are reconstructed using the same algorithms used for data.

4 Corrections and backgrounds

The MC simulations are corrected to improve the modeling of the data. First, weight factors are applied to all simulated events to match the pileup distribution in data, which consists of roughly 20 interactions per crossing. These weights are based on the measured instantaneous luminosity and the total inelastic cross section that provides a good description of the average number of reconstructed vertices.

The total lepton-selection efficiency is factorized into the product of reconstruction, identification, isolation, and trigger efficiencies, with each component measured in samples of $Z/\gamma \to \ell^+\ell^-$ events through a "tag-and-probe" method [19,20], in bins of lepton p_T and η. A charge-dependent efficiency in the muon triggering and reconstruction was observed in previous CMS measurements [35]. In the muon channel, all efficiencies are therefore determined separately for positively and negatively charged muons. The same procedures are used for data as for the simulated events, and scale factors are extracted to match the simulated event-selection efficiencies to those in the data.

The lepton momentum is calibrated using $Z/\gamma \to \ell^+\ell^-$ events [36]. The dominant sources of the mismeasurement of muon momentum originate from the mismodeling of tracker alignment and of the magnetic field. The correction parameters are obtained in bins of muon η and ϕ. First, the average $1/p_T$ values of the reconstructed muon curvature in data and simulation are corrected to the corresponding values calculated for MC generated muons. Then, using MC simulation, the resolution in the reconstructed muon momentum is parametrized as a function of the muon p_T in bins of muon

$|\eta|$ and the number of tracker hits used in the reconstruction. Next, the correction parameters of the muon momentum scale are fine-tuned by matching the average dimuon mass in each bin of muon charge, η, and ϕ to their reference values. At this point, the "reference" distributions, which are based on the generated muons, are smeared by the reconstruction resolution derived in the previous step. Finally, the scale factors for the muon momentum resolution, in bins of muon $|\eta|$, are determined by fitting the "reference" dimuon mass distribution to data.

A similar procedure is followed for electrons to reduce the small residual difference between the data and MC simulation. Unlike for muons, the measured electron energy is dominated by the calorimeter, and the corrections are extracted identically for electrons and positrons. The electron energy-scale parameters are fine-tuned by correcting the average dielectron mass in each bin of electron η and ϕ to the corresponding "reference" values. Here, the "reference" distributions are based on the generated electrons (post FSR), combined with the FSR photons in a cone, and smeared by the reconstructed energy resolution.

The EW and top quark backgrounds are estimated using MC simulations based on the cross sections calculated at next-to-the-next-to-leading order in QCD [37,38] and normalized to the integrated luminosity. We use cross sections calculated at NLO for the diboson backgrounds. The multijet background in dimuon events, dominated by muons from heavy-flavor hadron decays, is evaluated using same-sign (SS) dimuon events. A small EW and top quark contamination is evaluated in an MC simulation and subtracted from the SS sample. The distributions are then scaled by roughly a factor of 2, estimated from simulated events, to obtain the multijet contamination in the signal OS dimuon sample. The multijet background in the dielectron analysis is evaluated using the SS sample in combination with the eμ events to subtract the contribution from the OS events caused by the misidentification of charge. The distributions used to estimate the background from jets misidentified as leptons (that include the multijet and W+jet events) are obtained from the SS eμ sample. These distributions are used to fit the dielectron mass distribution in the SS events in each $y_{\ell\ell}$ bin to extract the normalization of this background.

The dilepton mass and $\cos\theta^*$ distributions in three of the six rapidity bins are shown in Figs. 2 and 3, respectively. The figures include lepton momentum and efficiency corrections, background samples normalized as described above, and the signal normalized to the total expected number of events in the data.
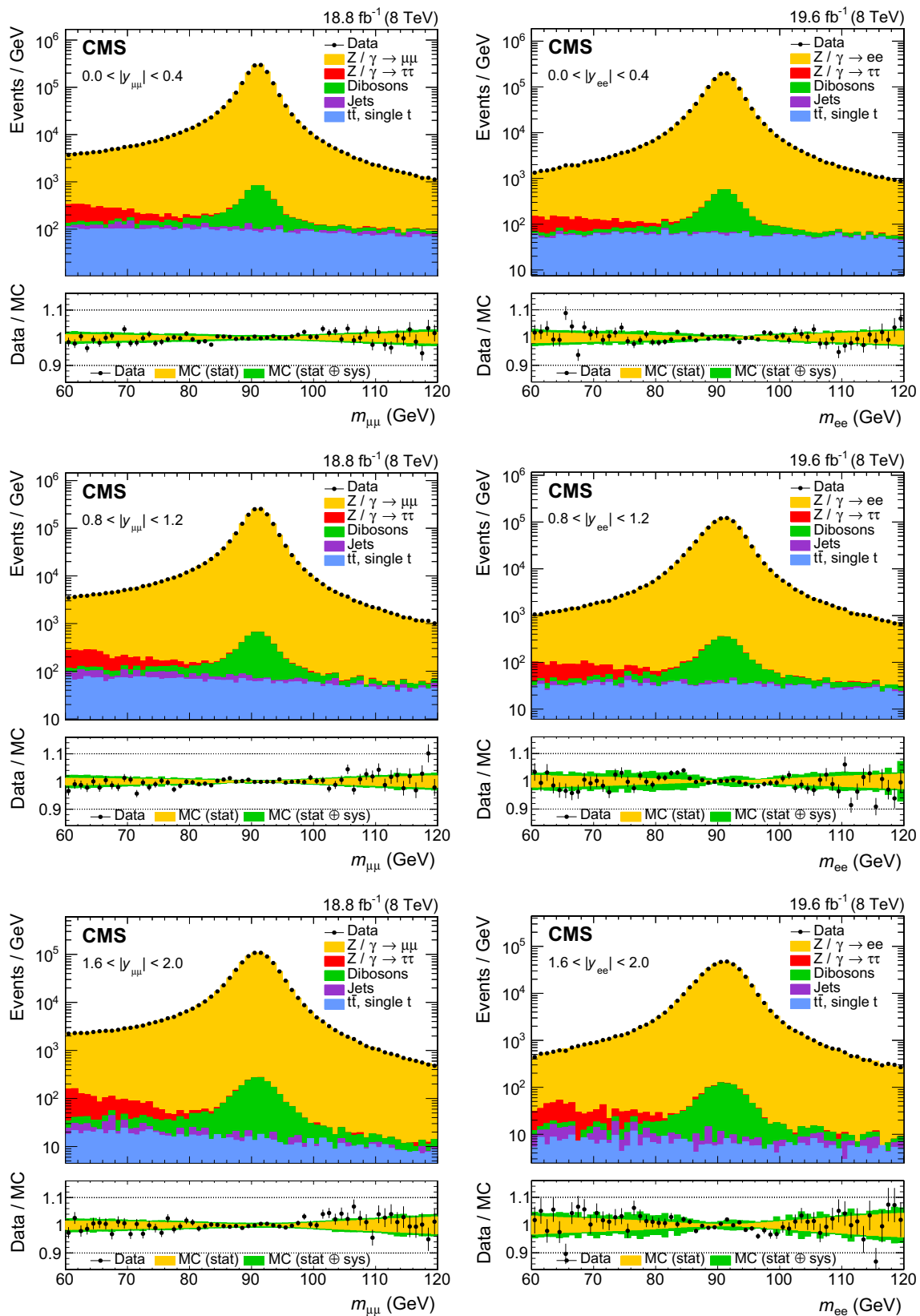
Fig. 2 Dimuon (left) and dielectron (right) mass distributions in three representative bins in rapidity: $|y_{\ell\ell}| < 0.4$ (upper), $0.8 < |y_{\ell\ell}| < 1.2$ (middle), and $1.6 < |y_{\ell\ell}| < 2.0$ (lower)
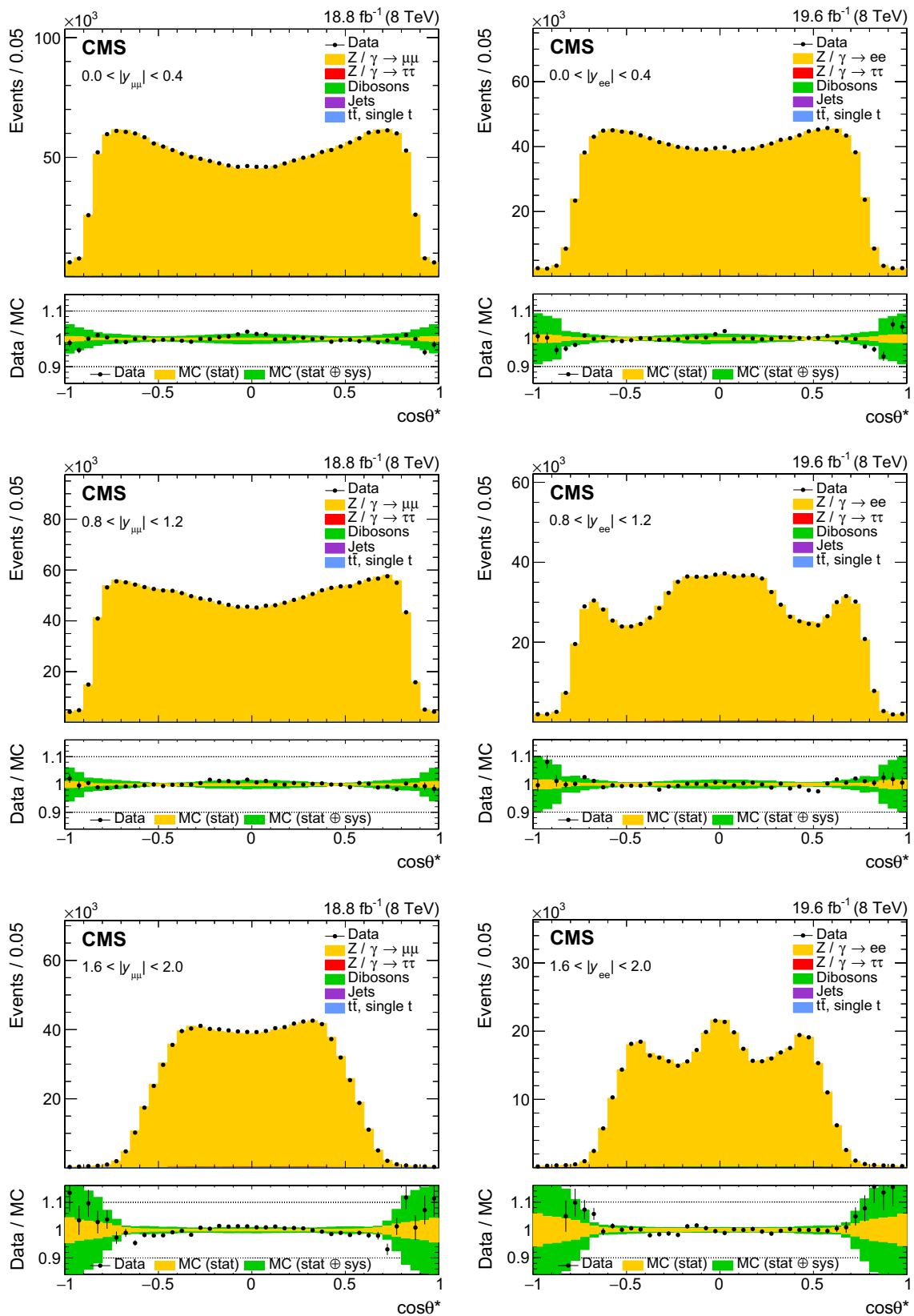
Fig. 3 The muon (left) and electron (right) $\cos\theta^*$ distributions in three representative bins in rapidity: $|y_{\ell\ell}| < 0.4$ (upper), $0.8 < |y_{\ell\ell}| < 1.2$ (middle), and $1.6 < |y_{\ell\ell}| < 2.0$ (lower). The small contributions from backgounds are included in the predictions

5 Weighted A_{FB} measurement

As introduced in Sect. 1, the LO angular distribution of dilepton events has a $(1 + \cos^2 \theta^*)$ term that arises from the spin-1 of the exchanged boson and a $\cos \theta^*$ term that originates from the interference between vector and axial-vector contributions. However, there is also a $(1 - 3 \cos^2 \theta^*)$ NLO term that originates from the p_T of the interacting partons [39]. Each $(m_{\ell\ell}, y_{\ell\ell})$ bin of the dilepton pair at NLO therefore has an angular distribution in $\cos \theta^*$ that follows the form [39]:

$$\frac{1}{\sigma} \frac{d\sigma}{d \cos \theta^*} = \frac{3}{8} \left[1 + \cos^2 \theta^* + \frac{A_0}{2}(1 - 3\cos^2 \theta^*) + A_4 \cos \theta^* \right].$$
(7)

The A_{FB} value in each $(m_{\ell\ell}, y_{\ell\ell})$ bin is calculated using the "angular event weighting" method, described in Ref. [40], in which each event with a $\cos \theta^*$ value (denoted as "c"), is reflected in the denominator (D) and numerator (N) weights through:

$$w_D = \frac{1}{2} \frac{c^2}{(1 + c^2 + h)^3},$$
(8)

$$w_N = \frac{1}{2} \frac{|c|}{(1 + c^2 + h)^2},$$
(9)

where $h = 0.5A_0(1 - 3c^2)$. Here, as a baseline we use the $p_{T,\ell\ell}$-averaged A_0 value of about 0.1 in each measurement $(m_{\ell\ell}, y_{\ell\ell})$ bin, as predicted by the signal MC simulation. Using the weighted sums N and D for forward ($\cos \theta^* > 0$) and backward ($\cos \theta^* < 0$) events, we obtain

$$D_F = \sum_{c>0} w_D, \quad D_B = \sum_{c<0} w_D,$$
(10)

$$N_F = \sum_{c>0} w_N, \quad N_B = \sum_{c<0} w_N,$$
(11)

from which the weighted A_{FB} of Eq. (2) can be written as:

$$A_{FB} = \frac{3}{8} \frac{N_F - N_B}{D_F + D_B}.$$
(12)

The statistical uncertainty in this weighted A_{FB} value takes into account correlations among the numerator and denominator sums. For data, the background contribution in the event-weighted sums are subtracted before calculating A_{FB}. In the full phase space, the values of the weighted and the nominal A_{FB}, calculated as an asymmetry between the total event counts in the forward and backward hemispheres, are the same. Since the acceptances of the forward and backward events are equal for same values of $|\cos \theta^*|$, the fiducial values of the event-weighted A_{FB} are also the same as in the full phase space, while the nominal A_{FB} values are smaller because of the limited acceptance at large $\cos \theta^*$. This feature makes an event-weighted A_{FB} less sensitive than the nominal

A_{FB} to the specific modeling of the acceptance. In addition, because the event-weighted A_{FB} exploits the full distribution in $\cos \theta^*$, as opposed to only its sign in the nominal A_{FB}, it therefore provides a smaller statistical uncertainty.

6 Extraction of $\sin^2 \theta_{eff}^\ell$

We extract $\sin^2 \theta_{eff}^\ell$ by fitting the A_{FB} $(m_{\ell\ell}, y_{\ell\ell})$ distribution in data with the theoretical predictions. The default signal distributions are based on the POWHEG v2 event generator using the NNPDF3.0 PDFs [17]. The POWHEG generator is interfaced with PYTHIA 8 [16] and the CUETP8M1 [31] underlying event tune to provide parton showering and hadronization, including electromagnetic FSR. The dependence on $\sin^2 \theta_{eff}^\ell$, on the renormalization and factorization scales, and on the PDFs is modeled through the POWHEG MC generator that provides matrix-element-based, event-by-event weights for each change in these parameters. The distributions are modified to different values of $\sin^2 \theta_{eff}^\ell$ by weighting each event in the full simulation by the ratio of $\cos \theta^*$ distributions obtained with the modified and default configurations in each $(m_{\ell\ell}, y_{\ell\ell})$ bin. The uncertainties in the simulation of the detector have a small effect because A_{FB} is extracted through the angular event-weighting technique that is insensitive to efficiency and acceptance.

Table 1 summarizes the statistical uncertainty in the extracted $\sin^2 \theta_{eff}^\ell$ in the muon and electron channels and in their combination. Comparisons between the data and best-fit distributions are shown in Fig. 4. The statistical uncertainties are evaluated through the bootstrapping technique [41], and take account of correlations among the measured A_{FB}, lepton selection efficiencies, and calibration coefficients introduced through the repeated use of the same dilepton events. We generate 400 pseudo-experiments that provide an accurate estimate of the statistical uncertainties and correlations. In each pseudo-experiment, every event in the data is replicated n times, where n is a random number sampled from a Poisson distribution with a mean of unity. All steps of the analysis, including extraction of muon selection efficiencies, calibration coefficients, and a measurement of A_{FB}, are performed for each pseudo-experiment. The statistical uncertainties in electron-selection efficiencies and calibration coefficients,

Table 1 Summary of statistical uncertainties in $\sin^2 \theta_{eff}^\ell$. The statistical uncertainties in the lepton-selection efficiency and in the calibration coefficients in data are included in the estimates

Channel	Statistical uncertainty
Muons	0.00044
Electrons	0.00060
Combined	0.00036

Fig. 4 Comparison between data and best-fit A_{FB} distributions in the dimuon (upper) and dielectron (lower) channels. The best-fit A_{FB} value in each bin is obtained via linear interpolation between two neighboring templates. Here, the templates are based on the central prediction of the NLO NNPDF3.0 PDFs. The error bars represent the statistical uncertainties in the data
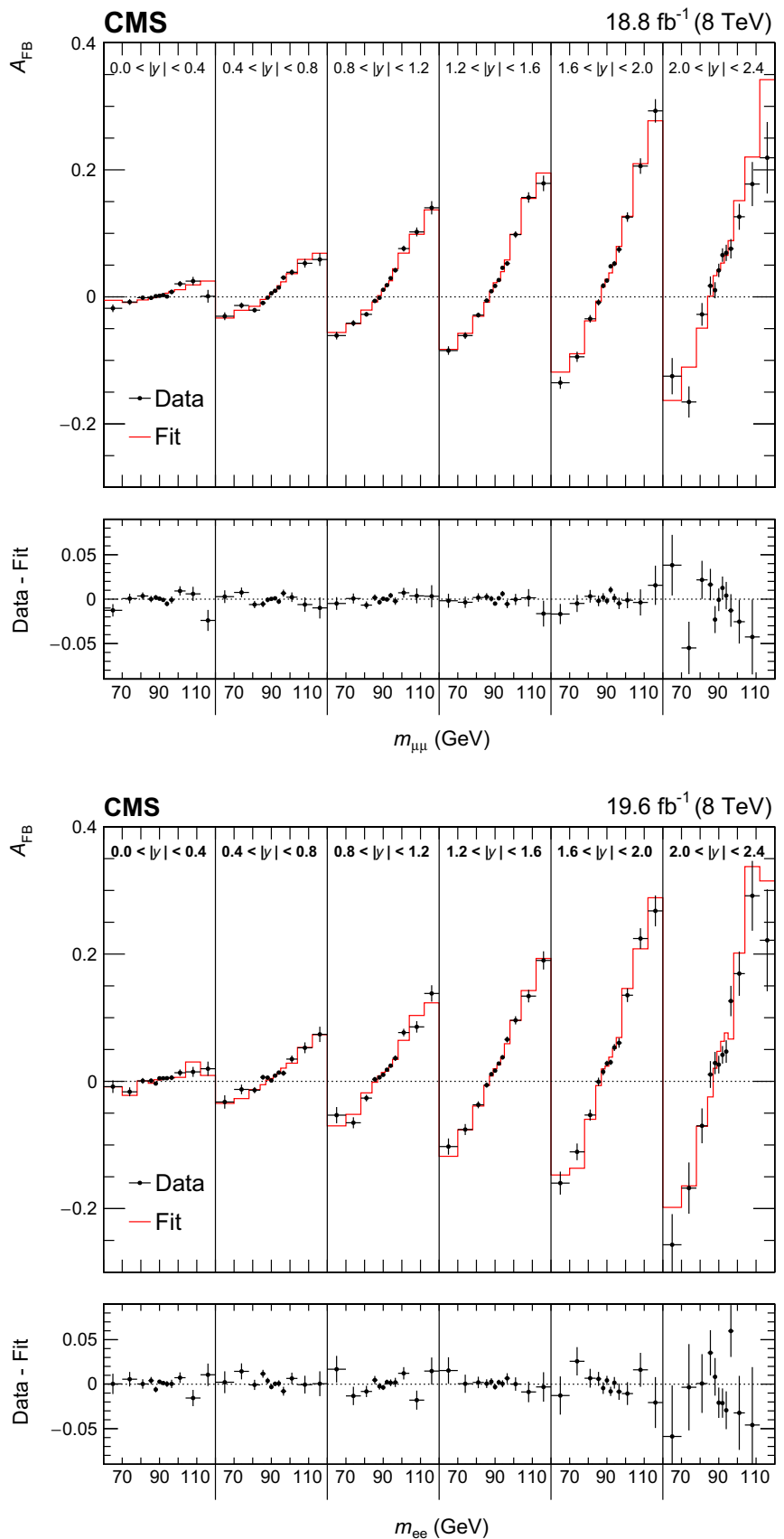
which have no charge dependence, are small and are evaluated separately.

7 Experimental systematic uncertainties

The experimental sources of systematic uncertainty reflect the statistical uncertainties in the simulated events, corrections to lepton-selection efficiency, and to the lepton-momentum scale and resolution, background subtraction, and modeling of pileup. For electrons, the selection efficiencies, which have no dependence on charge, cancel to first order, since we are using the angular event-weighting technique.

7.1 Statistical uncertainties in MC simulated events

To reduce the statistical uncertainties associated with the limited number of events in the signal MC samples, which include simulation of detector response and lepton reconstruction, the generated $\cos \theta^*$ distributions in each ($m_{\ell\ell}$, $y_{\ell\ell}$) bin within the acceptance of the detector is reweighted to much larger MC samples, generated without simulating detector response or lepton reconstruction. This makes the fluctuations in the generated $\cos \theta^*$ distributions negligible, and therefore the statistical uncertainties in the reconstructed A_{FB} values become dominated by fluctuations in the simulated detector response and lepton reconstruction. These uncertainties are evaluated using the bootstrapping [41] method in both dimuon and dielectron channels, described in Sect. 6, by reweighting the generated $\cos \theta^*$ distributions in each of the bootstrap samples. The total statistical uncertainties in the simulated events also include contributions from uncertainties in the measured lepton-selection efficiencies and calibration coefficients.

7.2 Lepton selection efficiencies

Several sources of uncertainty are considered in measuring of efficiencies. The statistical uncertainties in the lepton-selection efficiencies, evaluated through studies of pseudo-experiments, are included in the combined statistical uncertainty of the measured $\sin^2 \theta_{\text{eff}}^{\ell}$.

Combined scale factors for muon reconstruction, identification, and isolation efficiencies are changed by 0.5%, and trigger-selection efficiency scale factors by 0.2%, coherently for all bins for both positive and negative lepton charges. These take into account uncertainties associated with the tag-and-probe method, and are evaluated by changing signal and background models for dimuon mass distributions, levels of backgrounds, the dimuon mass range, and binning used in the fits. These uncertainties are considered fully correlated between the two charges, and therefore have a negligible impact on the measurement of $\sin^2 \theta_{\text{eff}}^{\ell}$. In addition, we assign the difference between the offline efficiencies obtained by fitting the dimuon mass distributions to extract the signal yields, and those found using simple counting method, as additional systematic uncertainties. The total systematic uncertainty in $\sin^2 \theta_{\text{eff}}^{\ell}$ originating from the muon selection efficiency is ±0.00005.

In a similar way as for muons, the scale factors for electron reconstruction, identification, and trigger-selection efficiencies are changed coherently within their uncertainties in all (p_{T}, η) bins, and the corresponding changes in the resulting $\sin^2 \theta_{\text{eff}}^{\ell}$ are assigned as systematic uncertainties. The total uncertainty in $\sin^2 \theta_{\text{eff}}^{\ell}$ originating from all electron efficiency-related systematic sources is ±0.00004.

7.3 Lepton momentum calibration

The statistical uncertainties in the parameters used to calibrate lepton momentum, described in Sect. 4, are included in the combined statistical uncertainty. The theoretical uncertainties, discussed in Sect. 8, are also propagated to the reference distributions used to extract the coefficients in the lepton momentum calibration.

When evaluating the average dimuon masses to extract the (η, ϕ) dependent corrections, the dimuon mass window is restricted to $86 < m_{\mu\mu} < 96$ GeV. This range of ±5 GeV centered at 91 GeV is changed from ±2.5 to ±10 GeV in steps of 0.5 GeV, and the full calibration sequence is repeated each time. Similarly, a dimuon mass window of ±10 (i.e., 81–101) GeV, used in the dimuon fits to obtain the resolution-correction factors, is changed from ±5 to ±25 GeV in steps of 1 GeV. For each of these modifications, the maximum deviation in the extracted $\sin^2 \theta_{\text{eff}}^{\ell}$ relative to the nominal configuration is taken as a systematic uncertainty. The total experimental systematic uncertainty in $\sin^2 \theta_{\text{eff}}^{\ell}$ originating from the muon-momentum calibration, evaluated by adding individual uncertainties in quadrature, is ±0.00008. The effects due to PDF uncertainties in the calibration coefficients were found to be negligible. In studies of the impact of the value of $\sin^2 \theta_{\text{eff}}^{\ell}$ used to generate the reference distributions for muon-momentum calibration over the range of $\Delta \sin^2 \theta_{\text{eff}}^{\ell} = 0.02000$, the extracted result changes at most by ±0.00008 due to the changes made in the muon-calibration parameters. Since the uncertainty in $\sin^2 \theta_{\text{eff}}^{\ell}$ is much smaller than ±0.02000, we conclude that this effect is negligible.

Similarly, the windows in the dielectron invariant mass used to extract the electron momentum-correction factors are changed to estimate the corresponding systematic uncertainty. And consider additional independent sources of systematic uncertainty from the modeling of pileup, background estimation, and bias in the dielecton mass-fitting procedure. The size of the EW corrections in the extracted electron

energy-calibration coefficients is estimated by modifying reference dielectron mass distributions through the weight factors obtained with ZGRAD [42]. All these systematic uncertainties are found to be rather small. The dominant uncertainty originates from the full corrections to the electron energy resolution, which improve the agreement between data and simulated dielectron mass distributions. The total systematic uncertainty in the extracted value of $\sin^2\theta_{\rm eff}^\ell$ due to both the electron energy scale and resolution is ± 0.00019.

7.4 Background

The systematic uncertainties in the estimated background are evaluated as follows. The normalizations of the top quark and $Z/\gamma \to \tau^+\tau^-$ backgrounds are changed respectively by 10 and 20%, covering the maximum deviations between the data and simulation observed in the eμ control region. The uncertainty in the multijet and W+jets background is estimated by changing them by $\pm 100\%$. Changing the diboson background prediction by 100% provides a negligible change in the result (<0.00001). Changing all EW and top quark backgrounds by the uncertainty in the integrated luminosity of 2.6% [43] also produces a negligible change in the result (<0.00001). The total systematic uncertainty in the measured $\sin^2\theta_{\rm eff}^\ell$ from the uncertainty in the background estimation is ± 0.00003 and ± 0.00005 in the dimuon and dielectron channels, respectively.

7.5 Pileup

To take into account the uncertainty originating from differences in pileup between data and simulation, we change the total inelastic cross section by $\pm 5\%$, and recompute the expected pileup distribution in data. The analysis is repeated and the difference relative to the central value is taken as the systematic uncertainty. These uncertainties are respectively ± 0.00003 and ± 0.00002 in the dimuon and dielectron channels.

All the above systematic uncertainties are summarized in Table 2.

8 Theoretical systematic uncertainties

We investigate sources of systematic uncertainty in modeling the MC templates. For each change in the model, we rederive the reference distributions described in Sect. 4 to adjust the lepton momentum calibration coefficients. As a baseline, the signal MC events are weighted to match the $p_{\rm T,\ell\ell}$ distribution in each $|y_{\ell\ell}|$ bin in the data. The difference relative to the result obtained without applying the weight factors, which is 0.00003 in both channels, is assigned as a systematic uncertainty associated with the modeling of $p_{\rm T,\ell\ell}$.

Table 2 Summary of experimental systematic uncertainties in $\sin^2\theta_{\rm eff}^\ell$

Source	Muons	Electrons
Size of MC event sample	0.00015	0.00033
Lepton selection efficiency	0.00005	0.00004
Lepton momentum calibration	0.00008	0.00019
Background subtraction	0.00003	0.00005
Modeling of pileup	0.00003	0.00002
Total	0.00018	0.00039

The renormalization and factorization scales, $\mu_{\rm R}$ and $\mu_{\rm F}$, are each changed independently by a factor of 2, up and down, such that their ratio is within $0.5 < \mu_{\rm R}/\mu_{\rm F} < 2.0$. The maximum deviation among these six variants relative to the nominal choice (excluding the two opposite changes) is assigned as a systematic uncertainty associated with the missing higher-order QCD correction terms.

In addition, we use a multi-scale improved NLO (MiNLO [44]) calculation for the Z+1 jet partonic final state (henceforth referred to as "Z+j"), interfaced with PYTHIA 8 for parton showering, FSR, and hadronization, to assess the uncertainty from the missing higher-order QCD terms and modeling of the angular coefficients. The MiNLO Z+j process has NLO accuracy for both Z+0 and Z+1 jet events, which provides a better description of the dependence of the angular coefficients on $p_{\rm T,\ell\ell}$.

Systematic uncertainties in modeling electromagnetic FSR are estimated by comparing results obtained with distributions based on PYTHIA 8 and PHOTOS 2.15 [45–47] for the modeling of FSR. Electroweak effects from the difference between the u and d quarks and leptonic effective mixing angles, are estimated by changing $\sin^2\theta_{\rm eff}^{\rm u}$ and $\sin^2\theta_{\rm eff}^{\rm d}$ by 0.0001 and 0.0002 [42], respectively, relative to $\sin^2\theta_{\rm eff}^\ell$. The $\sin^2\theta_{\rm eff}^\ell$ extracted using the corresponding distributions is shifted by 0.00001.

The underlying event tune parameters [31] are changed by their uncertainties, and $\sin^2\theta_{\rm eff}^\ell$ is extracted also using the corresponding distributions. The maximum difference from the default tune is taken as the corresponding uncertainty. The systematic uncertainties from these and all the above sources, are summarized in Table 3.

We also separately study the modeling of the A_0 angular coefficient, which is included in the definition of $A_{\rm FB}$. As a baseline, the $p_{\rm T,\ell\ell}$-averaged A_0 value in each measurement ($m_{\ell\ell}$, $y_{\ell\ell}$) bin is used in the definition of the weighted $A_{\rm FB}$. Several other options are studied: (i) the LO expression: $A_0 = p_{\rm T,\ell\ell}^2/(p_{\rm T,\ell\ell}^2 + m_{\ell\ell}^2)$, (ii) the $p_{\rm T,\ell\ell}$-dependent A_0 in each ($m_{\ell\ell}$, $y_{\ell\ell}$) bin as predicted in the baseline NLO POWHEG simulation, (iii) the $p_{\rm T,\ell\ell}$-dependent A_0 predicted in the MiNLO Z+j POWHEG generator, and (iv) A_0 set to 0. The same definition is used for data and simulation, and

Table 3 Summary of the theoretical uncertainties for the dimuon and dielectron channels, as discussed in the text

Modeling parameter	Muons	Electrons
Dilepton p_{T} reweighting	0.00003	0.00003
μ_{R} and μ_{F} scales	0.00011	0.00013
POWHEG MINLO Z+j $vs.$ Z at NLO	0.00009	0.00009
FSR model (PHOTOS $vs.$ PYTHIA 8)	0.00003	0.00005
Underlying event	0.00003	0.00004
Electroweak $\sin^2 \theta^{\ell}_{\mathrm{eff}}$ $vs.$ $\sin^2 \theta^{\mathrm{u,d}}_{\mathrm{eff}}$	0.00001	0.00001
Total	0.00015	0.00017

the extracted $\sin^2 \theta^{\ell}_{\mathrm{eff}}$ is identical within ± 0.00002 of the default. In addition, we weight the $|\cos \theta^*|$ distribution from the MINLO Z+j MC sample to match the dependence of A_0 on $p_{\mathrm{T},\ell\ell}$ in each $(m_{\ell\ell}, y_{\ell\ell})$ bin to the corresponding values of the baseline MC simulation. The change in the resulting $\sin^2 \theta^{\ell}_{\mathrm{eff}}$ is also negligible.

9 Uncertainties in the PDFs

The observed A_{FB} values depend on the size of the dilution effect, as well as on the relative contributions from u and d valence quarks to the total dilepton production cross section. The uncertainties in the PDFs translate into sizable changes in the observed A_{FB} values. However, changes in PDFs affect the $A_{\mathrm{FB}}(m_{\ell\ell}, y_{\ell\ell})$ distribution in a different way than changes in $\sin^2 \theta^{\ell}_{\mathrm{eff}}$.

Changes in PDFs produce large changes in A_{FB}, when the absolute values of A_{FB} are large, i.e., at large and small dilepton mass values. In contrast, the effect of changes in $\sin^2 \theta^{\ell}_{\mathrm{eff}}$ are largest near the Z boson peak, and are significantly smaller at high and low masses. Because of this behavior, which is illustrated in Fig. 5, we apply a Bayesian χ^2 reweighting method to constrain the PDFs [48–50], and thereby reduce their uncertainties in the extracted value of $\sin^2 \theta^{\ell}_{\mathrm{eff}}$.

As a baseline, we use the NLO NNPDF3.0 PDFs. In the Bayesian χ^2 reweighting method, PDF replicas that offer good descriptions of the observed A_{FB} distribution are assigned large weights, and those that poorly describe the A_{FB} are given small weights. Each weight factor is based on the best-fit $\chi^2_{\mathrm{min},i}$ value obtained by fitting the $A_{\mathrm{FB}}(m_{\ell\ell}, y_{\ell\ell})$ distribution with a given PDF replica i:

$$w_i = \frac{e^{-\frac{\chi^2_{\mathrm{min},i}}{2}}}{\frac{1}{N}\sum_{i=1}^{N} e^{-\frac{\chi^2_{\mathrm{min},i}}{2}}}, \tag{13}$$

where N is the number of replicas in a set of PDFs. The final result is then calculated as a weighted average over the
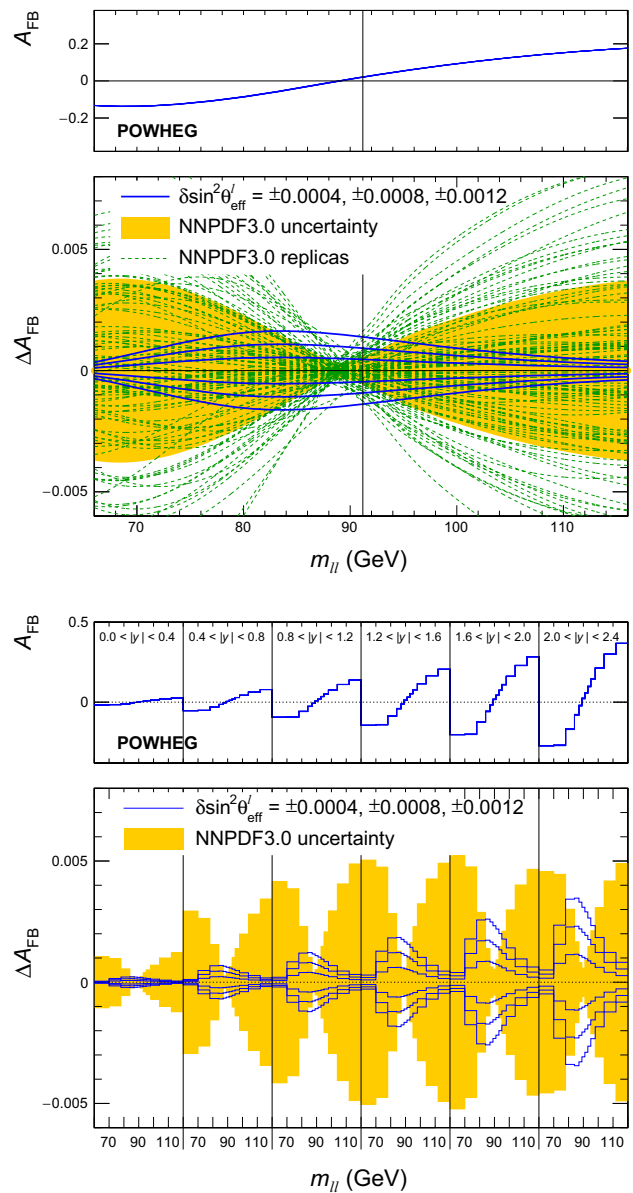

Fig. 5 Distribution in A_{FB} as a function of dilepton mass, integrated over rapidity (top), and in six rapidity bins (bottom) for $\sin^2 \theta^{\ell}_{\mathrm{eff}} = 0.23120$ in POWHEG. The solid lines in the bottom panel correspond to six changes at $\sin^2 \theta^{\ell}_{\mathrm{eff}}$ around the central value, corresponding to: ± 0.00040, ± 0.00080, and ± 0.00120. The dashed lines refer to the A_{FB} predictions for 100 NNPDF3.0 replicas. The shaded bands illustrate the standard deviation in the NNPDF3.0 replicas

replicas: $\sin^2 \theta^{\ell}_{\mathrm{eff}} = \sum_{i=1}^{N} w_i s_i / N$, where s_i is the best-fit $\sin^2 \theta^{\ell}_{\mathrm{eff}}$ value obtained for the ith replica.

Figure 6 shows a scatter plot of the χ^2_{min} $vs.$ the best-fit $\sin^2 \theta^{\ell}_{\mathrm{eff}}$ value for the 100 NNPDF3.0 replicas for the $\mu\mu$ and ee samples, and for the combined dimuon and dielectron results. All sources of statistical and experimental systematic uncertainties are included in a 72×72 covariance matrices for data and template A_{FB} distributions. The $\chi^2(s)$ is defined as:
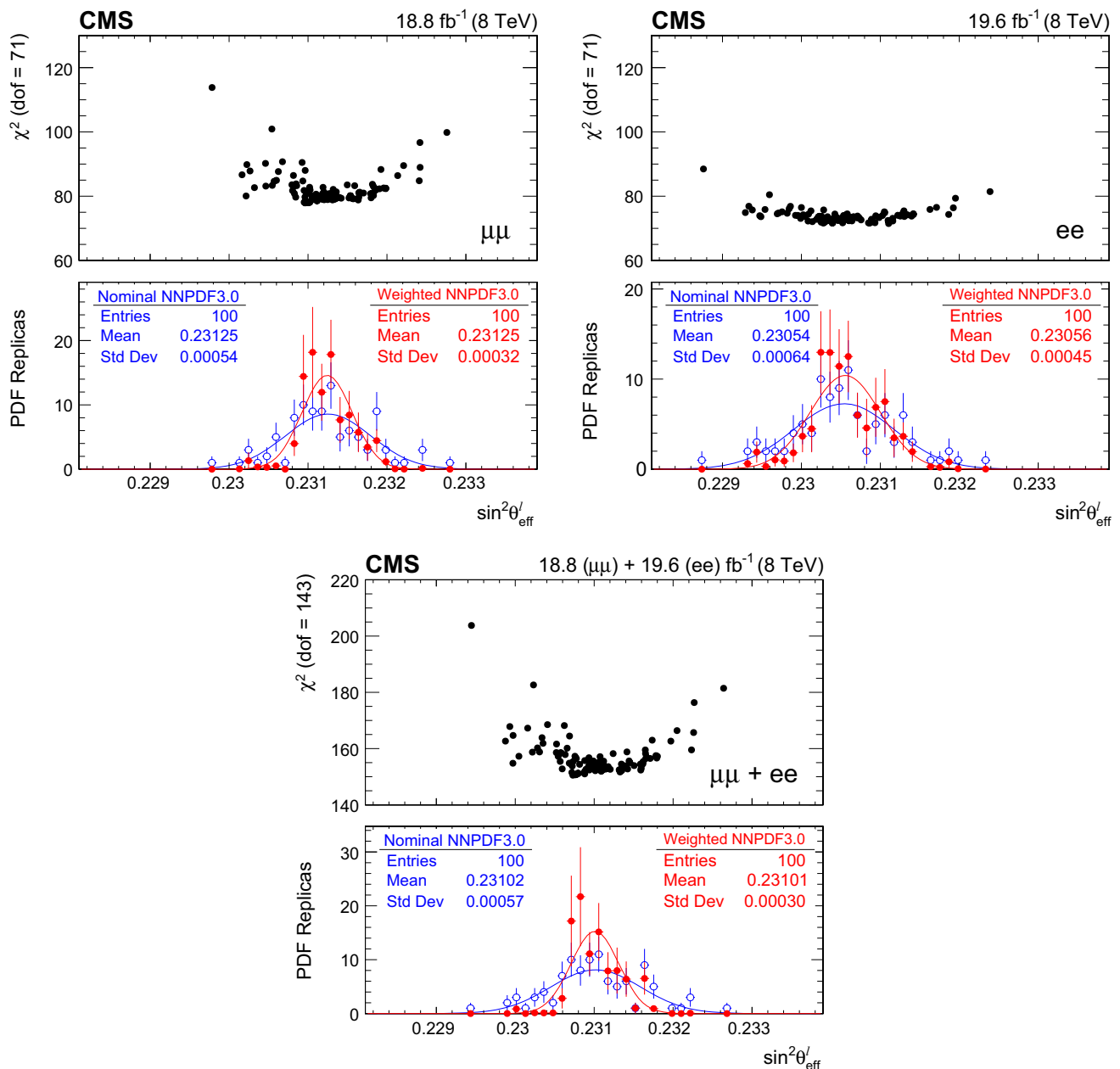
Fig. 6 The upper panel in each figure shows a scatter plot in $\chi^2_{\min}$ *vs.* the best-fit $\sin^2 \theta^\ell_{\text{eff}}$ for 100 NNPDF replicas in the muon channel (upper left), electron channel (upper right), and their combination (below). The corresponding lower panels have the projected distributions in the best-fit $\sin^2 \theta^\ell_{\text{eff}}$ for the nominal (open circles) and weighted (solid circles) replicas

$$\chi^2(s) = (\boldsymbol{D} - \boldsymbol{T}(s))^T \boldsymbol{V}^{-1} (\boldsymbol{D} - \boldsymbol{T}(s)), \tag{14}$$

where $\boldsymbol{D}$ represents the measured A_{FB} values for data in 72 bins, $\boldsymbol{T}(s)$ denotes the theoretical predictions for A_{FB} as a function of s, or $\sin^2 \theta^\ell_{\text{eff}}$, and $\boldsymbol{V}$ represents the sum of the covariance matrices for the data and templates. As illustrated in these figures, the extreme PDF replicas from either side are disfavored by both the dimuon and dielectron data. For each of the NNPDF3.0 replicas, the muon and electron results are

combined using their respective best-fit χ^2 values, $\sin^2 \theta^\ell_{\text{eff}}$, and their fitted statistical and experimental systematic uncertainties.

Figure 7 shows the extracted $\sin^2 \theta^\ell_{\text{eff}}$ in the muon and electron decay channels and their combination, with and without constraining the uncertainties in the PDFs. The corresponding numerical values are also listed in Table 4. After Bayesian χ^2 reweighting, the PDF uncertainties are reduced by about a factor of 2. It should be noted that the Bayesian χ^2 reweight-
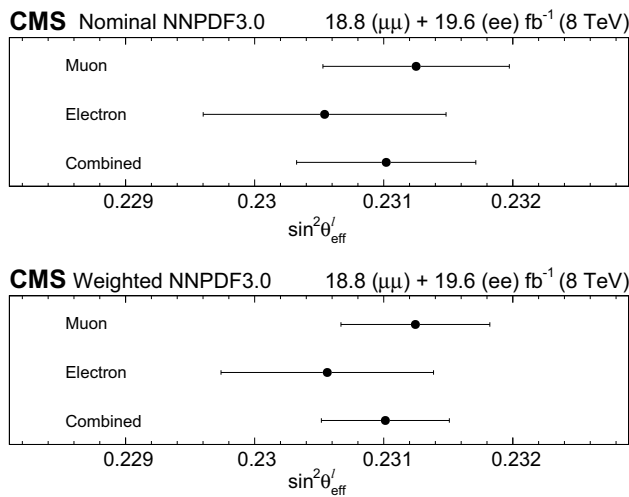
Fig. 7 The extracted values of $\sin^2 \theta_{\text{eff}}^{\ell}$ in the muon and electron channels, and their combination. The horizontal bars include statistical, experimental, and PDF uncertainties. The PDF uncertainties are obtained both without (top) and with (bottom) using the Bayesian χ^2 weighting
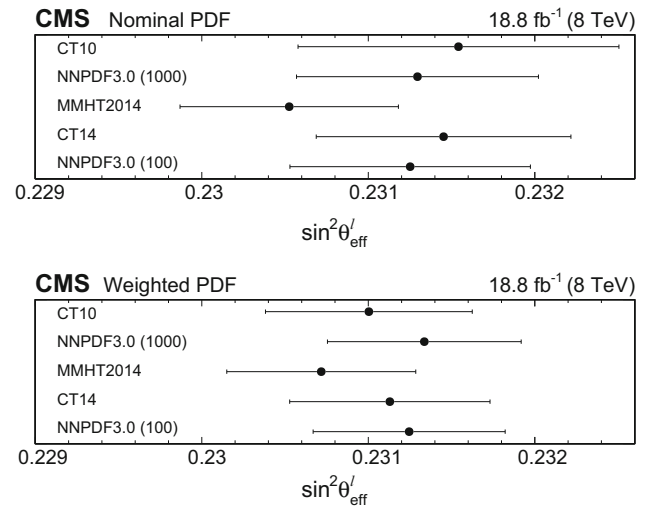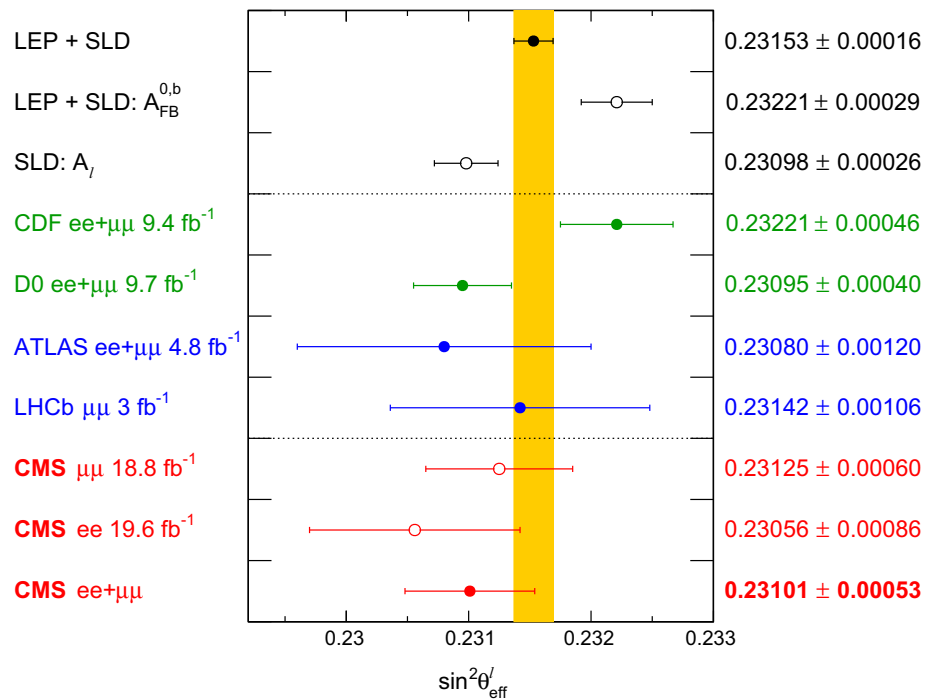

Fig. 8 Extracted values of $\sin^2 \theta_{\text{eff}}^{\ell}$ from the dimuon data for different sets of PDFs with the nominal (top) and χ^2-reweighted (bottom) replicas. The horizontal error bars include contributions from statistical, experimental, and PDF uncertainties

Table 4 The central value and the PDF uncertainty in the measured $\sin^2 \theta_{\text{eff}}^{\ell}$ in the muon and electron channels, and their combination, obtained without and with constraining PDFs using Bayesian χ^2 reweighting

Channel	Not constraining PDFs	Constraining PDFs
Muons	0.23125 ± 0.00054	0.23125 ± 0.00032
Electrons	0.23054 ± 0.00064	0.23056 ± 0.00045
Combined	0.23102 ± 0.00057	0.23101 ± 0.00030

ing technique works well when the replicas span the optimal value on both of its sides. In addition, the effective number of replicas after χ^2 reweighting, $n_{\text{eff}} = N^2 / \sum_{i=1}^{N} w_i^2$, should also be large enough to give a reasonable estimate of the average value and its standard deviation. There are 39 effective replicas after the χ^2 reweighting ($n_{\text{eff}} = 39$). Including the corresponding statistical uncertainty of 0.00005, the total PDF uncertainty becomes 0.00031. As a cross-check, we perform the analysis with the corresponding set of 1000 NNPDF3.0 replicas in the dimuon channel, and find good consistency between the two results.

We have also studied the PDFs represented by Hessian eigenvectors using the CT10 [28], CT14 [51], and MMHT2014 [52] PDFs in an analysis performed in the dimuon channel. First, we generate the replica predictions (i) for each observable O for the Hessian eigensets (k):

$$O_i = O_0 + \frac{1}{2} \sum_{k=0}^{n} (O_{2k+1} - O_{2k+2}) R_{ik}, \tag{15}$$

where n is the number of eigenvector axes, and the R_{ik} are random numbers sampled from the normal distribution with a mean of 0 and a standard deviation of unity. Then, the same technique is applied as used in the NNPDF analysis. The results of fits for these PDFs are summarized in Fig. 8. After Bayesian χ^2 reweighting the central predictions for all PDFs are closer to each other, and the corresponding uncertainties are significantly reduced. The result using CT14 is within about 1/3 of the PDF uncertainty of the NNPDF3.0 result in the muon channel, whereas the MMHT2014 set yields a smaller $\sin^2 \theta_{\text{eff}}^{\ell}$ value by about one standard deviation. Some of these differences can be reduced by adding more data (e.g. including the electron channel, which is not considered in this check). Some can be attributed to the residual differences in the valence and sea quark distributions, which are not fully constrained using the A_{FB} distributions alone. For example, we find that the NLO NNPDF3.0 PDF set yields a very good description for the published 8 TeV CMS muon charge asymmetry (χ^2 of 4.6 for 11 dof). In contrast, the χ^2 values with the CT14 and MMHT2014 PDF sets are 21.3 and 21.4, respectively. We also constructed a combined set from same number of replicas of NNPDF3.0, CT14, and MMHT2014 PDFs, and after including the data from the W charge asymmetry in the PDF reweighting, we find the combined weighted average in the dimuon channel differs from the NNPDF3.0 result by only 0.00009, and the standard deviation only increases from 0.00032 to 0.00036. Consequently, for our quoted results we use only the NNPDF3.0 PDF set, which is used in both dimuon and dielectron analyses.

As an additional test, for the case of Hessian PDFs (including the Hessian NNPDF3.0 [53]) we perform a simultaneous χ^2 fit for $\sin^2 \theta_{\text{eff}}^{\ell}$ and all PDF nuisance parameters repre-

Fig. 9 Comparison of the measured $\sin^2 \theta_{\mathrm{eff}}^{\ell}$ in the muon and electron channels and their combination, with previous LEP, SLD, Tevatron, and LHC measurements. The shaded band corresponds to the combination of the LEP and SLD measurements

LEP + SLD	0.23153 ± 0.00016
LEP + SLD: $A_{\mathrm{FB}}^{0,b}$	0.23221 ± 0.00029
SLD: A_l	0.23098 ± 0.00026
CDF ee+$\mu\mu$ 9.4 fb^{-1}	0.23221 ± 0.00046
D0 ee+$\mu\mu$ 9.7 fb^{-1}	0.23095 ± 0.00040
ATLAS ee+$\mu\mu$ 4.8 fb^{-1}	0.23080 ± 0.00120
LHCb $\mu\mu$ 3 fb^{-1}	0.23142 ± 0.00106
CMS $\mu\mu$ 18.8 fb^{-1}	0.23125 ± 0.00060
CMS ee 19.6 fb^{-1}	0.23056 ± 0.00086
CMS ee+$\mu\mu$	**0.23101 ± 0.00053**

senting the variations for each eigenvector. As expected for Gaussian distributions, we obtain the same central values and the total uncertainties that are extracted from Bayesian reweighting of the corresponding set of replicas.

Finally, as a cross-check, we also repeat the measurement using different mass windows for extracting $\sin^2 \theta_{\mathrm{eff}}^{\ell}$, and for constraining the PDFs. Specifically, we first use the central five bins, corresponding to the dimuon mass range of $84 < m_{\mu\mu} < 95$ GeV, to extract $\sin^2 \theta_{\mathrm{eff}}^{\ell}$. Then, we use predictions based on the extracted $\sin^2 \theta_{\mathrm{eff}}^{\ell}$ in the lower three ($60 < m_{\mu\mu} < 84$ GeV) and the higher four ($95 < m_{\mu\mu} < 120$ GeV) dimuon mass bins, to constrain the PDFs. We find that the statistical uncertainty increases by only about 10%, and the PDF uncertainty increases by only about 6% relative to the uncertainties obtained when using the full mass range to extract the $\sin^2 \theta_{\mathrm{eff}}^{\ell}$ and simultaneously constrain the PDFs. The test thereby confirms that the PDF uncertainties are constrained mainly by the high- and low-mass bins, and that we obtain consistent results with these two approaches.

10 Summary

The effective leptonic mixing angle, $\sin^2 \theta_{\mathrm{eff}}^{\ell}$, has been extracted from measurements of the mass and rapidity dependence of the forward–backward asymmetries A_{FB} in Drell–Yan $\mu\mu$ and ee production. As a baseline model, we use the POWHEG event generator for the inclusive pp $\rightarrow Z/\gamma \rightarrow \ell\ell$ process at leading electroweak order, where the weak mixing

angle is interpreted through the improved Born approximation as the effective angle incorporating higher-order corrections. With more data and new analysis techniques, including precise lepton-momentum calibration, angular event weighting, and additional constraints on PDFs, the statistical and systematic uncertainties are significantly reduced relative to previous CMS measurements. The combined result from the dielectron and dimuon channels is:

$$\sin^2 \theta_{\mathrm{eff}}^{\ell} = 0.23101 \pm 0.00036\,(\mathrm{stat}) \pm 0.00018\,(\mathrm{syst})$$
$$\pm 0.00016\,(\mathrm{theo}) \pm 0.00031\,(\mathrm{PDF}), \qquad (16)$$

or summing the uncertainties in quadrature,

$$\sin^2 \theta_{\mathrm{eff}}^{\ell} = 0.23101 \pm 0.00053. \qquad (17)$$

A comparison of the extracted $\sin^2 \theta_{\mathrm{eff}}^{\ell}$ with previous results from LEP, SLC, Tevatron, and LHC, shown in Fig. 9, indicates consistency with the mean of the most precise LEP and SLD results, as well as with the other measurements.

References

1. J.C. Collins, D.E. Soper, Angular distribution of dileptons in high-energy hadron collisions. Phys. Rev. D **16**, 2219 (1977). https://doi.org/10.1103/PhysRevD.16.2219

2. D.Y. Bardin, W.F.L. Hollik, G. Passarino, Reports of the working group on precision calculations for the z resonance. Technical report, CERN (1995). https://doi.org/10.5170/CERN-1995-003

3. D.Y. Bardin, ZFITTER v. 6.21: a semianalytical program for fermion pair production in e^+e^- annihilation. Comput. Phys. Commun. **133**, 229 (2001). https://doi.org/10.1016/S0010-4655(00)00152-1. arXiv:hep-ph/9908433

4. The ALEPH Collaboration, the DELPHI Collaboration, the L3 Collaboration, the OPAL Collaboration, the SLD Collaboration, the LEP Electroweak Working Group, the SLD Electroweak and Heavy Flavour Groups, Precision electroweak measurements on the Z resonance. Phys. Rept. **427**, 257 (2006). https://doi.org/10.1016/j.physrep.2005.12.006. arXiv:hep-ex/0509008

5. Collaboration, Measurement of the forward–backward charge asymmetry and extraction of $\sin^2\theta_W^{\rm eff}$ in p$\bar{\rm p}$ → Z/γ^* + X → e^+e^- + X events produced at $\sqrt{s}$ = 1.96 TeV. Phys. Rev. Lett. **101**, 191801 (2008). https://doi.org/10.1103/PhysRevLett.101.191801. arXiv:0804.3220

6. D0 Collaboration, Measurement of $\sin^2\theta_{\rm eff}^\ell$ and Z-light quark couplings using the forward-backward charge asymmetry in $p\bar{p}$ → Z/γ^* → e^+e^- events with $\mathcal{L}$ = 5.0 fb^{-1} at $\sqrt{s}$ = 1.96 TeV. Phys. Rev. D **84**, 012007 (2011). https://doi.org/10.1103/PhysRevD.84.012007. arXiv:1104.4590

7. CMS Collaboration, Measurement of the weak mixing angle with the Drell–Yan process in proton–proton collisions at the LHC. Phys. Rev. D **84**, 112002 (2011). https://doi.org/10.1103/PhysRevD.84.112002. arXiv:1110.2682

8. CDF Collaboration, Indirect measurement of $\sin^2\theta_W$ (M_W) using e^+e^- pairs in the Z-boson region with $p\bar{p}$ collisions at a center-of-momentum energy of 1.96 TeV. Phys. Rev. D **88**, 072002 (2013). https://doi.org/10.1103/PhysRevD.88.072002. arXiv:1307.0770

9. CDF Collaboration, Indirect measurement of $\sin^2\theta_W$ (or M_W) using $\mu^+\mu^-$ pairs from γ^*/Z bosons produced in $p\bar{p}$ collisions at a center-of-momentum energy of 1.96 TeV. Phys. Rev. D **89**, 072005 (2014). https://doi.org/10.1103/PhysRevD.89.072005. arXiv:1402.2239

10. D0 Collaboration, Measurement of the effective weak mixing angle in $p\bar{p}$ → Z/γ^* → e^+e^- events. Phys. Rev. Lett. **115**, 041801 (2015). https://doi.org/10.1103/PhysRevLett.115.041801. arXiv:1408.5016

11. ATLAS Collaboration, Measurement of the forward–backward asymmetry of electron and muon pair-production in pp collisions at $\sqrt{s}$ = 7 TeV with the ATLAS detector. JHEP **09**, 049 (2015). https://doi.org/10.1007/JHEP09(2015)049. arXiv:1503.03709

12. LHCb Collaboration, Measurement of the forward-backward asymmetry in Z/γ^* → $\mu^+\mu^-$ decays and determination of the effective weak mixing angle. JHEP **11**, 190 (2015). https://doi.org/10.1007/JHEP11(2015)190. arXiv:1509.07645

13. CDF Collaboration, Measurement of $\sin^2\theta_{\rm eff}^{\rm lept}$ using e^+e^- pairs from γ^*/Z bosons produced in $p\bar{p}$ collisions at a center-of-momentum energy of 1.96 TeV. Phys. Rev. D **93**, 112016 (2016). https://doi.org/10.1103/PhysRevD.93.112016. arXiv:1605.02719

14. D0 Collaboration, Measurement of the effective weak mixing angle in $p\bar{p}$ → Z/γ^* → $\ell^+\ell^-$ events. Phys. Rev. Lett. **120**, 241802 (2018). https://doi.org/10.1103/PhysRevLett.120.241802. arXiv:1710.03951

15. CDF and D0 Collaborations, Tevatron Run II combination of the effective leptonic electroweak mixing angle. arXiv:1801.06283. Submitted to Phys. Rev. D (2018)

16. T. Sjöstrand et al., An introduction to PYTHIA 8.2. Comput. Phys. Commun. **191**, 159 (2015). https://doi.org/10.1016/j.cpc.2015.01.024. arXiv:1410.3012

17. NNPDF Collaboration, Parton distributions for the LHC Run II. JHEP **04**, 040 (2015). https://doi.org/10.1007/JHEP04(2015)040. arXiv:1410.8849

18. CMS Collaboration, The CMS experiment at the CERN LHC. JINST **3**, S08004 (2008). https://doi.org/10.1088/1748-0221/3/08/S08004

19. CMS Collaboration, Performance of CMS muon reconstruction in pp collision events at $\sqrt{s}$ = 7 TeV. JINST **7**, P10002 (2012). https://doi.org/10.1088/1748-0221/7/10/P10002. arXiv:1206.4071

20. CMS Collaboration, Performance of electron reconstruction and selection with the CMS detector in proton–proton collisions at $\sqrt{s}$ = 8 TeV. JINST **10**, P06005 (2015). https://doi.org/10.1088/1748-0221/10/06/P06005. arXiv:1502.02701

21. CMS Collaboration, The CMS trigger system. JINST **12**, P01020 (2017). https://doi.org/10.1088/1748-0221/12/01/P01020. arXiv:1609.02366

22. CMS Collaboration, Particle-flow reconstruction and global event description with the CMS detector. JINST **12**, P10003 (2017) https://doi.org/10.1088/1748-0221/12/10/P10003. arXiv:1706.04965

23. D. Bourilkov, Photon-induced background for dilepton searches and measurements in pp collisions at 13 TeV, (2016). arXiv:1606.00523

24. S. Alioli, P. Nason, C. Oleari, E. Re, NLO vector-boson production matched with shower in POWHEG. JHEP **07**, 060 (2008). https://doi.org/10.1088/1126-6708/2008/07/060. arXiv:0805.4802

25. P. Nason, A new method for combining NLO QCD with shower Monte Carlo algorithms. JHEP **11**, 040 (2004). https://doi.org/10.1088/1126-6708/2004/11/040. arXiv:hep-ph/0409146

26. S. Frixione, P. Nason, C. Oleari, Matching NLO QCD computations with parton shower simulations: the POWHEG method. JHEP **11**, 070 (2007). https://doi.org/10.1088/1126-6708/2007/11/070. arXiv:0709.2092

27. S. Alioli, P. Nason, C. Oleari, E. Re, A general framework for implementing NLO calculations in shower Monte Carlo programs: the POWHEG BOX. JHEP **06**, 043 (2010). https://doi.org/10.1007/JHEP06(2010)043. arXiv:1002.2581

28. H.-L. Lai et al., New parton distributions for collider physics. Phys. Rev. D **82**, 074024 (2010). https://doi.org/10.1103/PhysRevD.82.074024. arXiv:1007.2241

29. T. Sjöstrand, S. Mrenna, P. Skands, PYTHIA 6.4 physics and manual. JHEP **05**, 026 (2006). https://doi.org/10.1088/1126-6708/2006/05/026. arXiv:hep-ph/0603175

30. CMS Collaboration, Study of the underlying event at forward rapidity in pp collisions at $\sqrt{s}$ = 0.9, 2.76, and 7 TeV. JHEP **04**, 072 (2013). https://doi.org/10.1007/JHEP04(2013)072. arXiv:1302.2394

31. CMS Collaboration, Event generator tunes obtained from underlying event and multiparton scattering measurements. Eur. Phys. J. C **76**, 155 (2016). https://doi.org/10.1140/epjc/s10052-016-3988-x. arXiv:1512.00815

32. N. Davidson et al., Universal interface of TAUOLA: technical and physics documentation. Comput. Phys. Commun. **183**, 821 (2012). https://doi.org/10.1016/j.cpc.2011.12.009. arXiv:1002.0543

33. J. Pumplin et al., New generation of parton distributions with uncertainties from global QCD analysis. JHEP **07**, 012 (2002). https://doi.org/10.1088/1126-6708/2002/07/012. arXiv:hep-ph/0201195

34. GEANT4 Collaboration, GEANT4—a simulation toolkit. Nucl. Instrum. Methods A **506**, 250 (2003). https://doi.org/10.1016/S0168-9002(03)01368-8

35. CMS Collaboration, Measurement of the differential cross section and charge asymmetry for inclusive pp → $W^{\pm}$ + X production at $\sqrt{s}$ = 8 TeV. Eur. Phys. J. C **76**, 469 (2016). https://doi.org/10.1140/epjc/s10052-016-4293-4. arXiv:1603.01803

36. A. Bodek et al., Extracting muon momentum scale corrections for hadron collider experiments. Eur. Phys. J. C **72**, 2194 (2012). https://doi.org/10.1140/epjc/s10052-012-2194-8. arXiv:1208.3710

37. Y. Li, F. Petriello, Combining QCD and electroweak corrections to dilepton production in the framework of the FEWZ simulation code. Phys. Rev. D **86**, 094034 (2012). https://doi.org/10.1103/PhysRevD.86.094034. arXiv:1208.5967

38. M. Czakon, A. Mitov, Top++: a program for the calculation of the top-pair cross-section at hadron colliders. Comput. Phys. Commun. **185**, 2930 (2014). https://doi.org/10.1016/j.cpc.2014.06.021. arXiv:1112.5675

39. E. Mirkes, J. Ohnemus, W and Z polarization effects in hadronic collisions. Phys. Rev. D **50**, 5692 (1994). https://doi.org/10.1103/PhysRevD.50.5692. arXiv:hep-ph/9406381

40. A. Bodek, A simple event weighting technique for optimizing the measurement of the forward–backward asymmetry of Drell–Yan dilepton pairs at hadron colliders. Eur. Phys. J. C **67**, 321 (2010). https://doi.org/10.1140/epjc/s10052-010-1287-5. arXiv:0911.2850

41. B. Efron, Bootstrap methods: another look at the jackknife. Ann. Stat. **7**, 1 (1979). https://doi.org/10.1214/aos/1176344552

42. U. Baur et al., Electroweak radiative corrections to neutral current Drell–Yan processes at hadron colliders. Phys. Rev. D **65**, 033007 (2002). https://doi.org/10.1103/PhysRevD.65.033007. arXiv:hep-ph/0108274

43. CMS Collaboration, CMS luminosity based on pixel cluster counting—summer 2013 update. Technical Report CMS-PAS-LUM-13-001 (2013). https://cds.cern.ch/record/1598864

44. K. Hamilton, P. Nason, G. Zanderighi, MINLO: multi-scale improved NLO. JHEP **10**, 155 (2012). https://doi.org/10.1007/JHEP10(2012)155. arXiv:1206.3572

45. P. Golonka, Z. Was, PHOTOS Monte Carlo: a precision tool for QED corrections in Z and W decays. Eur. Phys. J. C **45**, 97 (2006). https://doi.org/10.1140/epjc/s2005-02396-4. arXiv:hep-ph/0506026

46. E. Barberio, Z. Wąs, PHOTOS: a universal Monte Carlo for QED radiative corrections. Version 2.0. Comput. Phys. Commun. **79**, 291 (1994). https://doi.org/10.1016/0010-4655(94)90074-4

47. N. Davidson, T. Przedzinski, Z. Was, PHOTOS interface in C++: technical and physics documentation. Comput. Phys. Commun. **199**, 86 (2016). https://doi.org/10.1016/j.cpc.2015.09.013. arXiv:1011.0937

48. W.T. Giele, S. Keller, Implications of hadron collider observables on parton distribution function uncertainties. Phys. Rev. D **58**, 094023 (1998). https://doi.org/10.1103/PhysRevD.58.094023. arXiv:hep-ph/9803393

49. N. Sato, J.F. Owens, H. Prosper, Bayesian reweighting for global fits. Phys. Rev. D **89**, 114020 (2014). https://doi.org/10.1103/PhysRevD.89.114020. arXiv:1310.1089

50. A. Bodek, J. Han, A. Khukhunaishvili, W. Sakumoto, Using Drell–Yan forward–backward asymmetry to reduce PDF uncertainties in the measurement of electroweak parameters. Eur. Phys. J. C **76**, 115 (2016). https://doi.org/10.1140/epjc/s10052-016-3958-3. arXiv:1507.02470

51. S. Dulat, New parton distribution functions from a global analysis of quantum chromodynamics. Phys. Rev. D **93**, 033006 (2016). https://doi.org/10.1103/PhysRevD.93.033006. arXiv:1506.07443

52. L.A. Harland-Lang, A.D. Martin, P. Motylinski, R.S. Thorne, Parton distributions in the LHC era: MMHT, PDFs. Eur. Phys. J. C **75**(204), 2015 (2014). https://doi.org/10.1140/epjc/s10052-015-3397-6. arXiv:1412.3989

53. S. Carrazza, An unbiased Hessian representation for Monte Carlo PDFs. Eur. Phys. J. C **75**, 369 (2015). https://doi.org/10.1140/epjc/s10052-015-3590-7. arXiv:1505.06736

CMS Collaboration

Yerevan Physics Institute, Yerevan, Armenia
A. M. Sirunyan, A. Tumasyan

Institut für Hochenergiephysik, Vienna, Austria
W. Adam, F Ambrogi, E. Asilar, T. Bergauer, J. Brandstetter, E. Brondolin, M. Dragicevic, J. Erö, A. Escalante Del Valle,
M. Flechl, R. Frühwirth[1], V. M. Ghete, J. Hrubec, M. Jeitler[1], N. Krammer, I. Krätschmer, D. Liko, T. Madlener,
I. Mikulec, N. Rad, H. Rohringer, J. Schieck[1], R. Schöfbeck, M. Spanring, D. Spitzbart, A. Taurok, W. Waltenberger,
J. Wittmann, C.-E. Wulz[1], M. Zarucki

Institute for Nuclear Problems, Minsk, Belarus
V. Chekhovsky, V. Mossolov, J. SuarezGonzalez

Universiteit Antwerpen, Antwerp, Belgium
E. A. De Wolf, D. Di Croce, X. Janssen, J. Lauwers, M. Pieters, M. Van De Klundert, H. Van Haevermaet,
P. Van Mechelen, N. Van Remortel

Vrije Universiteit Brussel, Brussel, Belgium
S. Abu Zeid, F. Blekman, J. D'Hondt, I. De Bruyn, J. De Clercq, K. Deroover, G. Flouris, D. Lontkovskyi, S. Lowette,
I. Marchesini, S. Moortgat, L. Moreels, Q. Python, K. Skovpen, S. Tavernier, W. Van Doninck, P. Van Mulders, I. Van Parijs

Université Libre de Bruxelles, Brussels, Belgium
D. Beghin, B. Bilin, H. Brun, B. Clerbaux, G. De Lentdecker, H. Delannoy, B. Dorney, G. Fasanella, L. Favart,
R. Goldouzian, A. Grebenyuk, A. K. Kalsi, T. Lenzi, J. Luetic, N. Postiau, E. Starling, L. Thomas, C. Vander Velde,
P. Vanlaer, D. Vannerom, Q. Wang

Ghent University, Ghent, Belgium
T. Cornelis, D. Dobur, A. Fagot, M. Gul, I. Khvastunov[2], D. Poyraz, C. Roskas, D. Trocino, M. Tytgat, W. Verbeke,
B. Vermassen, M. Vit, N. Zaganidis

Université Catholique de Louvain, Louvain-la-Neuve, Belgium
H. Bakhshiansohi, O. Bondu, S. Brochet, G. Bruno, C. Caputo, P. David, C. Delaere, M. Delcourt, B. Francois,
A. Giammanco, G. Krintiras, V. Lemaitre, A. Magitteri, A. Mertens, M. Musich, K. Piotrzkowski, A. Saggio,
M. Vidal Marono, S. Wertz, J. Zobec

Centro Brasileiro de Pesquisas Fisicas, Rio de Janeiro, Brazil
F. L. Alves, G. A. Alves, L. Brito, G. Correia Silva, C. Hensel, A. Moraes, M. E. Pol, P. RebelloTeles

Universidade do Estado do Rio de Janeiro, Rio de Janeiro, Brazil
E. Belchior Batista DasChagas, W. Carvalho, J. Chinellato[3], E. Coelho, E. M. Da Costa, G. G. Da Silveira[4],
D. De Jesus Damiao, C. De Oliveira Martins, S. Fonseca De Souza, H. Malbouisson, D. Matos Figueiredo,
M. Melo De Almeida, C. Mora Herrera, L. Mundim, H. Nogima, W. L. Prado Da Silva, L. J. Sanchez Rosas, A. Santoro,
A. Sznajder, M. Thiel, E. J. TonelliManganote[3], F. Torres Da Silva DeAraujo, A. Vilela Pereira

Universidade Estadual Paulista[a], Universidade Federal do ABC[b], São Paulo, Brazil
S. Ahuja[a], C. A. Bernardes[a], L. Calligaris[a], T. R. FernandezPerez Tomei[a], E. M. Gregores[b], P. G. Mercadante[b],
S. F. Novaes[a], SandraS Padula[a], D. Romero Abad[b]

Institute for Nuclear Research and Nuclear Energy Bulgarian Academy of Sciences, Sofia, Bulgaria
A. Aleksandrov, R. Hadjiiska, P. Iaydjiev, A. Marinov, M. Misheva, M. Rodozov, M. Shopova, G. Sultanov

University of Sofia, Sofia, Bulgaria
A. Dimitrov, L. Litov, B. Pavlov, P. Petkov

Beihang University, Beijing, China
W. Fang[5], X. Gao[5], L. Yuan

Institute of High Energy Physics, Beijing, China
M. Ahmad, J. G. Bian, G. M. Chen, H. S. Chen, M. Chen, Y. Chen, C. H. Jiang, D. Leggat, H. Liao, Z. Liu, F. Romeo, S. M. Shaheen, A. Spiezia, J. Tao, C. Wang, Z. Wang, E. Yazgan, H. Zhang, J. Zhao

State Key Laboratory of Nuclear Physics and Technology, Peking University, Beijing, China
Y. Ban, G. Chen, J. Li, Q. Li, Y. Mao, S. J. Qian, D. Wang, Z. Xu

Tsinghua University, Beijing, China
Y. Wang

Universidad de Los Andes, Bogotá, Colombia
C. Avila, A. Cabrera, C. A. Carrillo Montoya, L. F. Chaparro Sierra, C. Florez, C. F. GonzálezHernández, M. A. Segura Delgado

University of Split, Faculty of Electrical Engineering, Mechanical Engineering and Naval Architecture, Split, Croatia
B. Courbon, N. Godinovic, D. Lelas, I. Puljak, T. Sculac

University of Split, Faculty of Science, Split, Croatia
Z. Antunovic, M. Kovac

Institute Rudjer Boskovic, Zagreb, Croatia
V. Brigljevic, D. Ferencek, K. Kadija, B. Mesic, A. Starodumov[6], T. Susa

University of Cyprus, Nicosia, Cyprus
M. W. Ather, A. Attikis, G. Mavromanolakis, J. Mousa, C. Nicolaou, F. Ptochos, P. A. Razis, H. Rykaczewski

Charles University, Prague, Czech Republic
M. Finger[7], M. Finger Jr.[7]

Escuela Politecnica Nacional, Quito, Ecuador
E. Ayala

Universidad San Francisco de Quito, Quito, Ecuador
E. Carrera Jarrin

Academy of Scientific Research and Technology of the Arab Republic of Egypt, Egyptian Network of High Energy Physics, Cairo, Egypt
A. Ellithi Kamel[8], A. Mohamed[9], E. Salama[10,11]

National Institute of Chemical Physics and Biophysics, Tallinn, Estonia
S. Bhowmik, A. Carvalho Antunes De Oliveira, R. K. Dewanjee, K. Ehataht, M. Kadastik, M. Raidal, C. Veelken

Department of Physics, University of Helsinki, Helsinki, Finland
P. Eerola, H. Kirschenmann, J. Pekkanen, M. Voutilainen

Helsinki Institute of Physics, Helsinki, Finland
J. Havukainen, J. K. Heikkilä, T. Järvinen, V. Karimäki, R. Kinnunen, T. Lampén, K. Lassila-Perini, S. Laurila, S. Lehti, T. Lindén, P. Luukka, T. Mäenpää, H. Siikonen, E. Tuominen, J. Tuominiemi

Lappeenranta University of Technology, Lappeenranta, Finland
T. Tuuva

IRFU, CEA, Université Paris-Saclay, Gif-sur-Yvette, France
M. Besancon, F. Couderc, M. Dejardin, D. Denegri, J. L. Faure, F. Ferri, S. Ganjour, A. Givernaud, P. Gras, G. Hamel de Monchenault, P. Jarry, C. Leloup, E. Locci, J. Malcles, G. Negro, J. Rander, A. Rosowsky, M. Ö. Sahin, M. Titov

Laboratoire Leprince-Ringuet, Ecole Polytechnique, CNRS/IN2P3, Université Paris-Saclay, Palaiseau, France
A. Abdulsalam[12], I. Antropov, F. Beaudette, P. Busson, C. Charlot, R. Granier de Cassagnac, I. Kucher, S. Lisniak, A. Lobanov, J. Martin Blanco, M. Nguyen, C. Ochando, G. Ortona, P. Pigard, R. Salerno, J. B. Sauvan, Y. Sirois, A. G. StahlLeiton, A. Zabi, A. Zghiche

Université de Strasbourg, CNRS, IPHC UMR 7178, Strasbourg, France

J.-L. Agram[13], J. Andrea, D. Bloch, J.-M. Brom, E. C. Chabert, V. Cherepanov, C. Collard, E. Conte[13], J.-C. Fontaine[13], D. Gelé, U. Goerlach, M. Jansová, A.-C. Le Bihan, N. Tonon, P. Van Hove

Centre de Calcul de l'Institut National de Physique Nucleaire et de Physique des Particules, CNRS/IN2P3, Villeurbanne, France

S. Gadrat

Université de Lyon, Université Claude Bernard Lyon 1, CNRS-IN2P3, Institut de Physique Nucléaire de Lyon, Villeurbanne, France

S. Beauceron, C. Bernet, G. Boudoul, N. Chanon, R. Chierici, D. Contardo, P. Depasse, H. El Mamouni, J. Fay, L. Finco, S. Gascon, M. Gouzevitch, G. Grenier, B. Ille, F. Lagarde, I. B. Laktineh, H. Lattaud, M. Lethuillier, L. Mirabito, A. L. Pequegnot, S. Perries, A. Popov[14], V. Sordini, M. Vander Donckt, S. Viret, S. Zhang

Georgian Technical University, Tbilisi, Georgia

T. Toriashvili[15]

Tbilisi State University, Tbilisi, Georgia

D. Lomidze

RWTH Aachen University, I. Physikalisches Institut, Aachen, Germany

C. Autermann, L. Feld, M. K. Kiesel, K. Klein, M. Lipinski, M. Preuten, M. P. Rauch, C. Schomakers, J. Schulz, M. Teroerde, B. Wittmer, V. Zhukov[14]

RWTH Aachen University, III. Physikalisches Institut A, Aachen, Germany

A. Albert, D. Duchardt, M. Endres, M. Erdmann, S. Erdweg, T. Esch, R. Fischer, S. Ghosh, A. Güth, T. Hebbeker, C. Heidemann, K. Hoepfner, H. Keller, S. Knutzen, L. Mastrolorenzo, M. Merschmeyer, A. Meyer, P. Millet, S. Mukherjee, T. Pook, M. Radziej, H. Reithler, M. Rieger, F. Scheuch, A. Schmidt, D. Teyssier, S. Thüer

RWTH Aachen University, III. Physikalisches Institut B, Aachen, Germany

G. Flügge, O. Hlushchenko, B. Kargoll, T. Kress, A. Künsken, T. Müller, A. Nehrkorn, A. Nowack, C. Pistone, O. Pooth, H. Sert, A. Stahl[16]

Deutsches Elektronen-Synchrotron, Hamburg, Germany

M. Aldaya Martin, T. Arndt, C. Asawatangtrakuldee, I. Babounikau, K. Beernaert, O. Behnke, U. Behrens, A. BermúdezMartínez, D. Bertsche, A. A. Bin Anuar, K. Borras[17], V. Botta, A. Campbell, P. Connor, C. Contreras-Campana, F. Costanza, V. Danilov, A. De Wit, M. M. Defranchis, C. Diez Pardos, D. Domínguez Damiani, G. Eckerlin, T. Eichhorn, A. Elwood, E. Eren, E. Gallo[18], A. Geiser, J. M. Grados Luyando, A. Grohsjean, P. Gunnellini, M. Guthoff, A. Harb, J. Hauk, H. Jung, M. Kasemann, J. Keaveney, C. Kleinwort, J. Knolle, D. Krücker, W. Lange, A. Lelek, T. Lenz, K. Lipka, W. Lohmann[19], R. Mankel, I.-A. Melzer-Pellmann, A. B. Meyer, M. Meyer, M. Missiroli, G. Mittag, J. Mnich, V. Myronenko, S. K. Pflitsch, D. Pitzl, A. Raspereza, M. Savitskyi, P. Saxena, P. Schütze, C. Schwanenberger, R. Shevchenko, A. Singh, N. Stefaniuk, H. Tholen, A. Vagnerini, G. P. Van Onsem, R. Walsh, Y. Wen, K. Wichmann, C. Wissing, O. Zenaiev

University of Hamburg, Hamburg, Germany

R. Aggleton, S. Bein, A. Benecke, V. Blobel, M. Centis Vignali, T. Dreyer, E. Garutti, D. Gonzalez, J. Haller, A. Hinzmann, M. Hoffmann, A. Karavdina, G. Kasieczka, R. Klanner, R. Kogler, N. Kovalchuk, S. Kurz, V. Kutzner, J. Lange, D. Marconi, J. Multhaup, M. Niedziela, D. Nowatschin, A. Perieanu, A. Reimers, O. Rieger, C. Scharf, P. Schleper, S. Schumann, J. Schwandt, J. Sonneveld, H. Stadie, G. Steinbrück, F. M. Stober, M. Stöver, D. Troendle, E. Usai, A. Vanhoefer, B. Vormwald

Karlsruher Institut fuer Technology, Karlsruhe, Germany

M. Akbiyik, C. Barth, M. Baselga, S. Baur, E. Butz, R. Caspart, T. Chwalek, F. Colombo, W. De Boer, A. Dierlamm, N. Faltermann, B. Freund, M. Giffels, M. A. Harrendorf, F. Hartmann[16], S. M. Heindl, U. Husemann, F. Kassel[16], I. Katkov[14], S. Kudella, H. Mildner, S. Mitra, M. U. Mozer, Th. Müller, M. Plagge, G. Quast, K. Rabbertz, M. Schröder, I. Shvetsov, G. Sieber, H. J. Simonis, R. Ulrich, S. Wayand, M. Weber, T. Weiler, S. Williamson, C. Wöhrmann, R. Wolf

Institute of Nuclear and Particle Physics (INPP), NCSR Demokritos, Aghia Paraskevi, Greece

G. Anagnostou, G. Daskalakis, T. Geralis, A. Kyriakis, D. Loukas, G. Paspalaki, I. Topsis-Giotis

National and Kapodistrian University of Athens, Athens, Greece
G. Karathanasis, S. Kesisoglou, P. Kontaxakis, A. Panagiotou, N. Saoulidou, E. Tziaferi, K. Vellidis

National Technical University of Athens, Athens, Greece
K. Kousouris, I. Papakrivopoulos, G. Tsipolitis

University of Ioánnina, Ioannina, Greece
I. Evangelou, C. Foudas, P. Gianneios, P. Katsoulis, P. Kokkas, S. Mallios, N. Manthos, I. Papadopoulos, E. Paradas, J. Strologas, F. A. Triantis, D. Tsitsonis

MTA-ELTE Lendület CMS Particle and Nuclear Physics Group, Eötvös Loránd University, Budapest, Hungary
M. Csanad, N. Filipovic, P. Major, M. I. Nagy, G. Pasztor, O. Surányi, G. I. Veres

Wigner Research Centre for Physics, Budapest, Hungary
G. Bencze, C. Hajdu, D. Horvath[20], Á. Hunyadi, F. Sikler, T. Á. Vámi, V. Veszpremi, G. Vesztergombi[†]

Institute of Nuclear Research ATOMKI, Debrecen, Hungary
N. Beni, S. Czellar, J. Karancsi[22], A. Makovec, J. Molnar, Z. Szillasi

Institute of Physics, University of Debrecen, Debrecen, Hungary
M. Bartók[21], P. Raics, Z. L. Trocsanyi, B. Ujvari

Indian Institute of Science (IISc), Bangalore, India
S. Choudhury, J. R. Komaragiri

National Institute of Science Education and Research, HBNI, Bhubaneswar, India
S. Bahinipati[23], P. Mal, K. Mandal, A. Nayak[24], D. K. Sahoo[23], S. K. Swain

Panjab University, Chandigarh, India
S. Bansal, S. B. Beri, V. Bhatnagar, S. Chauhan, R. Chawla, N. Dhingra, R. Gupta, A. Kaur, A. Kaur, M. Kaur, S. Kaur, R. Kumar, P. Kumari, M. Lohan, A. Mehta, S. Sharma, J. B. Singh, G. Walia

University of Delhi, Delhi, India
A. Bhardwaj, B. C. Choudhary, R. B. Garg, M. Gola, S. Keshri, Ashok Kumar, S. Malhotra, M. Naimuddin, P. Priyanka, K. Ranjan, Aashaq Shah, R. Sharma

Saha Institute of Nuclear Physics, HBNI, Kolkata, India
R. Bhardwaj[25], M. Bharti, R. Bhattacharya, S. Bhattacharya, U. Bhawandeep[25], D. Bhowmik, S. Dey, S. Dutta[25], S. Dutt, S. Ghosh, K. Mondal, S. Nandan, A. Purohit, P. K. Rout, A. Roy, S. Roy Chowdhury, S. Sarkar, M. Sharan, B. Singh, S. Thakur[25]

Indian Institute of Technology Madras, Chennai, India
P. K. Behera

Bhabha Atomic Research Centre, Mumbai, India
R. Chudasama, D. Dutta, V. Jha, V. Kumar, P. K. Netrakanti, L. M. Pant, P. Shukla

Tata Institute of Fundamental Research-A, Mumbai, India
T. Aziz, M. A. Bhat, S. Dugad, B. Mahakud, G. B. Mohanty, N. Sur, B. Sutar, RavindraKumar Verma

Tata Institute of Fundamental Research-B, Mumbai, India
S. Banerjee, S. Bhattacharya, S. Chatterjee, P. Das, M. Guchait, Sa. Jain, S. Kumar, M. Maity[26], G. Majumder, K. Mazumdar, N. Sahoo, T. Sarkar[26]

Indian Institute of Science Education and Research (IISER), Pune, India
S. Chauhan, S. Dube, V. Hegde, A. Kapoor, K. Kothekar, S. Pandey, A. Rane, S. Sharma

Institute for Research in Fundamental Sciences (IPM), Tehran, Iran
S. Chenarani[27], E. EskandariTadavani, S. M. Etesami[27], M. Khakzad, M. MohammadiNajafabadi, M. Naseri, F. Rezaei Hosseinabadi, B. Safarzadeh[28], M. Zeinali

University College Dublin, Dublin, Ireland

M. Felcini, M. Grunewald

INFN Sezione di Bari[a], Università di Bari[b], Politecnico di Bari[c], Bari, Italy

M. Abbrescia[a,b], C. Calabria[a,b], A. Colaleo[a], D. Creanza[a,c], L. Cristella[a,b], N. De Filippis[a,c], M. De Palma[a,b], A. Di Florio[a,b], F. Errico[a,b], L. Fiore[a], A. Gelmi[a,b], G. Iaselli[a,c], S. Lezki[a,b], G. Maggi[a,c], M. Maggi[a], G. Miniello[a,b], S. My[a,b], S. Nuzzo[a,b], A. Pompili[a,b], G. Pugliese[a,c], R. Radogna[a], A. Ranieri[a], G. Selvaggi[a,b], A. Sharma[a], L. Silvestris[a,16], R. Venditti[a], P. Verwilligen[a], G. Zito[a]

INFN Sezione di Bologna[a], Università di Bologna[b], Bologna, Italy

G. Abbiendi[a], C. Battilana[a,b], D. Bonacorsi[a,b], L. Borgonovi[a,b], S. Braibant-Giacomelli[a,b], L. Brigliadori[a,b], R. Campanini[a,b], P. Capiluppi[a,b], A. Castro[a,b], F. R. Cavallo[a], S. S. Chhibra[a,b], G. Codispoti[a,b], M. Cuffiani[a,b], G. M. Dallavalle[a], F. Fabbri[a], A. Fanfani[a,b], P. Giacomelli[a], C. Grandi[a], L. Guiducci[a,b], S. Marcellini[a], G. Masetti[a], A. Montanari[a], F. L. Navarria[a,b], A. Perrotta[a], A. M. Rossi[a,b], T. Rovelli[a,b], G. P. Siroli[a,b], N. Tosi[a]

INFN Sezione di Catania[a], Università di Catania[b], Catania, Italy

S. Albergo[a,b], A. Di Mattia[a], R. Potenza[a,b], A. Tricomi[a,b], C. Tuve[a,b]

INFN Sezione di Firenze[a], Università di Firenze[b], Florence, Italy

G. Barbagli[a], K. Chatterjee[a,b], V. Ciulli[a,b], C. Civinini[a], R. D'Alessandro[a,b], E. Focardi[a,b], G. Latino, P. Lenzi[a,b], M. Meschini[a], S. Paoletti[a], L. Russo[a,29], G. Sguazzoni[a], D. Strom[a], L. Viliani[a]

INFN Laboratori Nazionali di Frascati, Frascati, Italy

L. Benussi, S. Bianco, F. Fabbri, D. Piccolo, F. Primavera[16]

INFN Sezione di Genova[a], Università di Genova[b], Genoa, Italy

F. Ferro[a], F. Ravera[a,b], E. Robutti[a], S. Tosi[a,b]

INFN Sezione di Milano-Bicocca[a], Università di Milano-Bicocca[b], Milan, Italy

A. Benaglia[a], A. Beschi[b], L. Brianza[a,b], F. Brivio[a,b], V. Ciriolo[a,b,16], S. Di Guida[a,b,16], M. E. Dinardo[a,b], S. Fiorendi[a,b], S. Gennai[a], A. Ghezzi[a,b], P. Govoni[a,b], M. Malberti[a,b], S. Malvezzi[a], R. A. Manzoni[a,b], A. Massironi[a,b], D. Menasce[a], L. Moroni[a], M. Paganoni[a,b], D. Pedrini[a], S. Ragazzi[a,b], T. Tabarelli de Fatis[a,b]

INFN Sezione di Napoli[a], Università di Napoli 'Federico II'[b], Napoli, Italy, Università della Basilicata[c], Potenza, Italy, Università G. Marconi[d], Rome, Italy

S. Buontempo[a], N. Cavallo[a,c], A. Di Crescenzo[a,d], F. Fabozzi[a,c], F. Fienga[a,b], G. Galati[a,b], A. O. M. Iorio[a,b], W. A. Khan[a], L. Lista[a], S. Meola[a,d,16], P. Paolucci[a,16], C. Sciacca[a,b], E. Voevodina[a,b]

INFN Sezione di Padova[a], Università di Padova[b], Padova, Italy, Università di Trento[c], Trento, Italy

P. Azzi[a], N. Bacchetta[a], L. Benato[a,b], D. Bisello[a,b], A. Boletti[a,b], A. Bragagnolo[a,b], R. Carlin[a,b], P. Checchia[a], M. Dall'Osso[a,b], P. De Castro Manzano[a], T. Dorigo[a], U. Dosselli[a], U. Gasparini[a,b], A. Gozzelino[a], S. Lacaprara[a], P. Lujan, M. Margoni[a,b], A. T. Meneguzzo[a,b], N. Pozzobon[a,b], P. Ronchese[a,b], R. Rossin[a,b], F. Simonetto[a,b], A. Tiko, E. Torassa[a], M. Zanetti[a,b], P. Zotto[a,b], G. Zumerle[a,b]

INFN Sezione di Pavia[a], Università di Pavia[b], Pavia, Italy

A. Braghieri[a], A. Magnani[a], P. Montagna[a,b], S. P. Ratti[a,b], V. Re[a], M. Ressegotti[a,b], C. Riccardi[a,b], P. Salvini[a], I. Vai[a,b], P. Vitulo[a,b]

INFN Sezione di Perugia[a], Università di Perugia[b], Perugia, Italy

L. Alunni Solestizi[a,b], M. Biasini[a,b], G. M. Bilei[a], C. Cecchi[a,b], D. Ciangottini[a,b], L. Fanò[a,b], P. Lariccia[a,b], E. Manoni[a], G. Mantovani[a,b], V. Mariani[a,b], M. Menichelli[a], A. Rossi[a,b], A. Santocchia[a,b], D. Spiga[a]

INFN Sezione di Pisa[a], Università di Pisa[b], Scuola Normale Superiore di Pisa[c], Pisa, Italy

K. Androsov[a], P. Azzurri[a], L. Bianchini[a], L. Bernardini[a], T. Boccali[a], L. Borrello, R. Castaldi[a], M. A. Ciocci[a,b], R. Dell'Orso[a], G. Fedi[a], L. Giannini[a,c], A. Giassi[a], M. T. Grippo[a], F. Ligabue[a,c], E. Manca[a,c], G. Mandorli[a,c], A. Messineo[a,b], F. Palla[a], A. Rizzi[a,b], P. Spagnolo[a], R. Tenchini[a], G. Tonelli[a,b], A. Venturi[a], P. G. Verdini[a]

INFN Sezione di Roma[a], Università di Roma[b], Rome, Italy

L. Barone[a,b], F. Cavallari[a], M. Cipriani[a,b], N. Daci[a], D. Del Re[a,b], E. Di Marco[a,b], M. Diemoz[a], S. Gelli[a,b], E. Longo[a,b], B. Marzocchi[a,b], P. Meridiani[a], G. Organtini[a,b], F. Pandolfi[a], R. Paramatti[a,b], F. Preiato[a,b], S. Rahatlou[a,b], C. Rovelli[a], F. Santanastasio[a,b]

INFN Sezione di Torino[a], Università di Torino[b], Turin, Italy, Università del Piemonte Orientale[c], Novara, Italy

N. Amapane[a,b], R. Arcidiacono[a,c], S. Argiro[a,b], M. Arneodo[a,c], N. Bartosik[a], R. Bellan[a,b], C. Biino[a], N. Cartiglia[a], F. Cenna[a,b], M. Costa[a,b], R. Covarelli[a,b], N. Demaria[a], B. Kiani[a,b], C. Mariotti[a], S. Maselli[a], E. Migliore[a,b], V. Monaco[a,b], E. Monteil[a,b], M. Monteno[a], M. M. Obertino[a,b], L. Pacher[a,b], N. Pastrone[a], M. Pelliccioni[a], G. L. PinnaAngioni[a,b], A. Romero[a,b], M. Ruspa[a,c], R. Sacchi[a,b], K. Shchelina[a,b], V. Sola[a], A. Solano[a,b], A. Staiano[a]

INFN Sezione di Trieste[a], Università di Trieste[b], Trieste, Italy

S. Belforte[a], V. Candelise[a,b], M. Casarsa[a], F. Cossutti[a], G. Della Ricca[a,b], F. Vazzoler[a,b], A. Zanetti[a]

Kyungpook National University, Daegu, Korea

D. H. Kim, G. N. Kim, M. S. Kim, J. Lee, S. Lee, S. W. Lee, C. S. Moon, Y. D. Oh, S. Sekmen, D. C. Son, Y. C. Yang

Chonnam National University, Institute for Universe and Elementary Particles, Kwangju, Korea

H. Kim, D. H. Moon, G. Oh

Hanyang University, Seoul, Korea

J. Goh, T. J. Kim

Korea University, Seoul, Korea

S. Cho, S. Choi, Y. Go, D. Gyun, S. Ha, B. Hong, Y. Jo, K. Lee, K. S. Lee, S. Lee, J. Lim, S. K. Park, Y. Roh

Sejong University, Seoul, Korea

H. Kim

Seoul National University, Seoul, Korea

J. Almond, J. Kim, J. S. Kim, H. Lee, K. Lee, K. Nam, S. B. Oh, B. C. Radburn-Smith, S. h. Seo, U. K. Yang, H. D. Yoo, G. B. Yu

University of Seoul, Seoul, Korea

H. Kim, J. H. Kim, J. S. H. Lee, I. C. Park

Sungkyunkwan University, Suwon, Korea

Y. Choi, C. Hwang, J. Lee, I. Yu

Vilnius University, Vilnius, Lithuania

V. Dudenas, A. Juodagalvis, J. Vaitkus

National Centre for Particle Physics, Universiti Malaya, Kuala Lumpur, Malaysia

I. Ahmed, Z. A. Ibrahim, M. A. B. Md Ali[30], F. Mohamad Idris[31], W. A. T. Wan Abdullah, M. N. Yusli, Z. Zolkapli

Centro de Investigacion y de Estudios Avanzados del IPN, Mexico City, Mexico

M. C. Duran-Osuna, H. Castilla-Valdez, E. DeLa Cruz-Burelo, G. Ramirez-Sanchez, I. Heredia-DeLa Cruz[32], R. I. Rabadan-Trejo, R. Lopez-Fernandez, J. MejiaGuisao, R Reyes-Almanza, A. Sanchez-Hernandez

Universidad Iberoamericana, Mexico City, Mexico

S. Carrillo Moreno, C. OropezaBarrera, F. VazquezValencia

Benemerita Universidad Autonoma de Puebla, Puebla, Mexico

J. Eysermans, I. Pedraza, H. A. Salazar Ibarguen, C. UribeEstrada

Universidad Autónoma de San Luis Potosí, San Luis Potosí, Mexico

A. Morelos Pineda

University of Auckland, Auckland, New Zealand

D. Krofcheck

University of Canterbury, Christchurch, New Zealand
S. Bheesette, P. H. Butler

National Centre for Physics, Quaid-I-Azam University, Islamabad, Pakistan
A. Ahmad, M. Ahmad, M. I. Asghar, Q. Hassan, H. R. Hoorani, A. Saddique, M. A. Shah, M. Shoaib, M. Waqas

National Centre for Nuclear Research, Swierk, Poland
H. Bialkowska, M. Bluj, B. Boimska, T. Frueboes, M. Górski, M. Kazana, K. Nawrocki, M. Szleper, P. Traczyk,
P. Zalewski

Institute of Experimental Physics, Faculty of Physics, University of Warsaw, Warsaw, Poland
K. Bunkowski, A. Byszuk[33], K. Doroba, A. Kalinowski, M. Konecki, J. Krolikowski, M. Misiura, M. Olszewski,
A. Pyskir, M. Walczak

Laboratório de Instrumentação e Física Experimental de Partículas, Lisbon, Portugal
P. Bargassa, C. Beirão Da Cruz E. Silva, A. Di Francesco, P. Faccioli, B. Galinhas, M. Gallinaro, J. Hollar, N. Leonardo,
L. Lloret Iglesias, M. V. Nemallapudi, J. Seixas, G. Strong, O. Toldaiev, D. Vadruccio, J. Varela

Joint Institute for Nuclear Research, Dubna, Russia
M. Gavrilenko, A. Golunov, I. Golutvin, N. Gorbounov, I. Gorbunov, A. Kamenev, V. Karjavin, V. Korenkov, A. Lanev,
A. Malakhov, V. Matveev[34,35], P. Moisenz, V. Palichik, V. Perelygin, M. Savina, S. Shmatov, V. Smirnov, N. Voytishin,
A. Zarubin

Petersburg Nuclear Physics Institute, Gatchina, (St. Petersburg), Russia
V. Golovtsov, Y. Ivanov, V. Kim[36], E. Kuznetsova[37], P. Levchenko, V. Murzin, V. Oreshkin, I. Smirnov, D. Sosnov,
V. Sulimov, L. Uvarov, S. Vavilov, A. Vorobyev

Institute for Nuclear Research, Moscow, Russia
Yu. Andreev, A. Dermenev, S. Gninenko, N. Golubev, A. Karneyeu, M. Kirsanov, N. Krasnikov, A. Pashenkov, D. Tlisov,
A. Toropin

Institute for Theoretical and Experimental Physics, Moscow, Russia
V. Epshteyn, V. Gavrilov, N. Lychkovskaya, V. Popov, I. Pozdnyakov, G. Safronov, A. Spiridonov, A. Stepennov,
V. Stolin, M. Toms, E. Vlasov, A. Zhokin

Moscow Institute of Physics and Technology, Moscow, Russia
T. Aushev, A. Bylinkin[35]

National Research Nuclear University 'Moscow Engineering Physics Institute' (MEPhI), Moscow, Russia
M. Chadeeva[38], P. Parygin, D. Philippov, S. Polikarpov[38], E. Popova, V. Rusinov

P.N. Lebedev Physical Institute, Moscow, Russia
V. Andreev, M. Azarkin[35], I. Dremin[35], M. Kirakosyan[36], S. V. Rusakov, A. Terkulov

Skobeltsyn Institute of Nuclear Physics, Lomonosov Moscow State University, Moscow, Russia
A. Baskakov, A. Belyaev, E. Boos, V. Bunichev, M. Dubinin[39], L. Dudko, A. Ershov, A. Gribushin, V. Klyukhin,
O. Kodolova, I. Lokhtin, I. Miagkov, S. Obraztsov, V. Savrin, A. Snigirev

Novosibirsk State University (NSU), Novosibirsk, Russia
V. Blinov[40], T. Dimova[40], L. Kardapoltsev[40], D. Shtol[40], Y. Skovpen[40]

State Research Center of Russian Federation, Institute for High Energy Physics of NRC "Kurchatov Institute", Protvino, Russia
I. Azhgirey, I. Bayshev, S. Bitioukov, D. Elumakhov, A. Godizov, V. Kachanov, A. Kalinin, D. Konstantinov, P. Mandrik,
V. Petrov, R. Ryutin, S. Slabospitskii, A. Sobol, S. Troshin, N. Tyurin, A. Uzunian, A. Volkov

National Research Tomsk Polytechnic University, Tomsk, Russia
A. Babaev

University of Belgrade, Faculty of Physics and Vinca Institute of Nuclear Sciences, Belgrade, Serbia
P. Adzic[41], P. Cirkovic, D. Devetak, M. Dordevic, J. Milosevic

Centro de Investigaciones Energéticas Medioambientales y Tecnológicas (CIEMAT), Madrid, Spain
J. AlcarazMaestre, A. Álvarez Fernández, I. Bachiller, M. Barrio Luna, J. A. Brochero Cifuentes, M. Cerrada, N. Colino, B. DeLa Cruz, A. DelgadoPeris, C. Fernandez Bedoya, J. P. Fernández Ramos, J. Flix, M. C. Fouz, O. Gonzalez Lopez, S. Goy Lopez, J. M. Hernandez, M. I. Josa, D. Moran, A. Pérez-Calero Yzquierdo, J. PuertaPelayo, I. Redondo, L. Romero, M. S. Soares, A. Triossi

Universidad Autónoma de Madrid, Madrid, Spain
C. Albajar, J. F. de Trocóniz

Universidad de Oviedo, Oviedo, Spain
J. Cuevas, C. Erice, J. Fernandez Menendez, S. Folgueras, I. Gonzalez Caballero, J. R. González Fernández, E. Palencia Cortezon, V. Rodríguez Bouza, S. SanchezCruz, P. Vischia, J. M. Vizan Garcia

Instituto de Física de Cantabria (IFCA), CSIC-Universidad de Cantabria, Santander, Spain
I. J. Cabrillo, A. Calderon, B. Chazin Quero, J. Duarte Campderros, M. Fernandez, P. J. Fernández Manteca, A. García Alonso, J. Garcia-Ferrero, G. Gomez, A. LopezVirto, J. Marco, C. Martinez Rivero, P. Martinez Ruiz del Arbol, F. Matorras, J. Piedra Gomez, C. Prieels, T. Rodrigo, A. Ruiz-Jimeno, L. Scodellaro, N. Trevisani, I. Vila, R. VilarCortabitarte

CERN, European Organization for Nuclear Research, Geneva, Switzerland
D. Abbaneo, B. Akgun, E. Auffray, P. Baillon, A. H. Ball, D. Barney, J. Bendavid, M. Bianco, A. Bocci, C. Botta, T. Camporesi, M. Cepeda, G. Cerminara, E. Chapon, Y. Chen, G. Cucciati, D. d'Enterria, A. Dabrowski, V. Daponte, A. David, A. De Roeck, N. Deelen, M. Dobson, T. du Pree, M. Dünser, N. Dupont, A. Elliott-Peisert, P. Everaerts, F. Fallavollita[42], D. Fasanella, G. Franzoni, J. Fulcher, W. Funk, D. Gigi, A. Gilbert, K. Gill, F. Glege, D. Gulhan, J. Hegeman, V. Innocente, A. Jafari, P. Janot, O. Karacheban[19], J. Kieseler, V. Knünz, A. Kornmayer, M. Krammer[1], C. Lange, P. Lecoq, C. Lourenço, M. T. Lucchini, L. Malgeri, M. Mannelli, F. Meijers, J. A. Merlin, S. Mersi, E. Meschi, P. Milenovic[43], F. Moortgat, M. Mulders, H. Neugebauer, J. Ngadiuba, S. Orfanelli, L. Orsini, F. Pantaleo[16], L. Pape, E. Perez, M. Peruzzi, A. Petrilli, G. Petrucciani, A. Pfeiffer, M. Pierini, F. M. Pitters, D. Rabady, A. Racz, T. Reis, G. Rolandi[44], M. Rovere, H. Sakulin, C. Schäfer, C. Schwick, M. Seidel, M. Selvaggi, A. Sharma, P. Silva, P. Sphicas[45], A. Stakia, J. Steggemann, M. Tosi, D. Treille, A. Tsirou, V. Veckalns[46], M. Verweij, W. D. Zeuner

Paul Scherrer Institut, Villigen, Switzerland
W. Bertl[†], L. Caminada[47], K. Deiters, W. Erdmann, R. Horisberger, Q. Ingram, H. C. Kaestli, D. Kotlinski, U. Langenegger, T. Rohe, S. A. Wiederkehr

ETH Zurich - Institute for Particle Physics and Astrophysics (IPA), Zurich, Switzerland
M. Backhaus, L. Bäni, P. Berger, N. Chernyavskaya, G. Dissertori, M. Dittmar, M. Donegà, C. Dorfer, C. Grab, C. Heidegger, D. Hits, J. Hoss, T. Klijnsma, W. Lustermann, M. Marionneau, M. T. Meinhard, D. Meister, F. Micheli, P. Musella, F. Nessi-Tedaldi, J. Pata, F. Pauss, G. Perrin, L. Perrozzi, S. Pigazzini, M. Quittnat, M. Reichmann, D. Ruini, D. A. Sanz Becerra, M. Schönenberger, L. Shchutska, V. R. Tavolaro, K. Theofilatos, M. L. Vesterbacka Olsson, R. Wallny, D. H. Zhu

Universität Zürich, Zurich, Switzerland
T. K. Aarrestad, C. Amsler[48], D. Brzhechko, M. F. Canelli, A. De Cosa, R. Del Burgo, S. Donato, C. Galloni, T. Hreus, B. Kilminster, I. Neutelings, D. Pinna, G. Rauco, P. Robmann, D. Salerno, K. Schweiger, C. Seitz, Y. Takahashi, A. Zucchetta

National Central University, Chung-Li, Taiwan
V. Candelise, Y. H. Chang, K. y. Cheng, T. H. Doan, Sh. Jain, R. Khurana, C. M. Kuo, W. Lin, A. Pozdnyakov, S. S. Yu

National Taiwan University (NTU), Taipei, Taiwan
P. Chang, Y. Chao, K. F. Chen, P. H. Chen, W.-S. Hou, Arun Kumar, Y. y. Li, R.-S. Lu, E. Paganis, A. Psallidas, A. Steen, J. f. Tsai

Chulalongkorn University, Faculty of Science, Department of Physics, Bangkok, Thailand
B. Asavapibhop, N. Srimanobhas, N. Suwonjandee

Çukurova University, Physics Department, Science and Art Faculty, Adana, Turkey

A. Bat, F. Boran, S. Cerci[49], S. Damarseckin, Z. S. Demiroglu, C. Dozen, I. Dumanoglu, S. Girgis, G. Gokbulut, Y. Guler, E. Gurpinar, I. Hos[50], E. E. Kangal[51], O. Kara, A. Kayis Topaksu, U. Kiminsu, M. Oglakci, G. Onengut, K. Ozdemir[52], S. Ozturk[53], D. Sunar Cerci[49], B. Tali[49], U. G. Tok, S. Turkcapar, I. S. Zorbakir, C. Zorbilmez

Middle East Technical University, Physics Department, Ankara, Turkey

B. Isildak[54], G. Karapinar[55], M. Yalvac, M. Zeyrek

Bogazici University, Istanbul, Turkey

I. O. Atakisi, E. Gülmez, M. Kaya[56], O. Kaya[57], S. Tekten, E. A. Yetkin[58]

Istanbul Technical University, Istanbul, Turkey

M. N. Agaras, S. Atay, A. Cakir, K. Cankocak, Y. Komurcu, S. Sen[59]

Institute for Scintillation Materials of National Academy of Science of Ukraine, Kharkov, Ukraine

B. Grynyov

National Scientific Center, Kharkov Institute of Physics and Technology, Kharkov, Ukraine

L. Levchuk

University of Bristol, Bristol, UK

T. Alexander, F. Ball, L. Beck, J. J. Brooke, D. Burns, E. Clement, D. Cussans, O. Davignon, H. Flacher, J. Goldstein, G. P. Heath, H. F. Heath, L. Kreczko, D. M. Newbold[60], S. Paramesvaran, B. Penning, T. Sakuma, D. Smith, V. J. Smith, J. Taylor

Rutherford Appleton Laboratory, Didcot, UK

K. W. Bell, A. Belyaev[61], C. Brew, R. M. Brown, D. Cieri, D. J. A. Cockerill, J.A. Coughlan, K. Harder, S. Harper, J. Linacre, E. Olaiya, D. Petyt, C. H. Shepherd-Themistocleous, A. Thea, I. R. Tomalin, T. Williams, W. J. Womersley

Imperial College, London, UK

G. Auzinger, R. Bainbridge, P. Bloch, J. Borg, S. Breeze, O. Buchmuller, A. Bundock, S. Casasso, D. Colling, L. Corpe, P. Dauncey, G. Davies, M. Della Negra, R. Di Maria, Y. Haddad, G. Hall, G. Iles, T. James, M. Komm, C. Laner, L. Lyons, A.-M. Magnan, S. Malik, A. Martelli, J. Nash[62], A. Nikitenko[6], V. Palladino, M. Pesaresi, A. Richards, A. Rose, E. Scott, C. Seez, A. Shtipliyski, G. Singh, M. Stoye, T. Strebler, S. Summers, A. Tapper, K. Uchida, T. Virdee[16], N. Wardle, D. Winterbottom, J. Wright, S. C. Zenz

Brunel University, Uxbridge, UK

J. E. Cole, P. R. Hobson, A. Khan, P. Kyberd, C. K. Mackay, A. Morton, I. D. Reid, L. Teodorescu, S. Zahid

Baylor University, Waco, USA

A. Borzou, K. Call, J. Dittmann, K. Hatakeyama, H. Liu, C. Madrid, B. Mcmaster, N. Pastika, C. Smith

Catholic University of America, Washington, DC, USA

R. Bartek, A. Dominguez

The University of Alabama, Tuscaloosa, USA

A. Buccilli, S. I. Cooper, C. Henderson, P. Rumerio, C. West

Boston University, Boston, USA

D. Arcaro, T. Bose, D. Gastler, D. Rankin, C. Richardson, J. Rohlf, L. Sulak, D. Zou

Brown University, Providence, USA

G. Benelli, X. Coubez, D. Cutts, M. Hadley, J. Hakala, U. Heintz, J. M. Hogan[63], K. H. M. Kwok, E. Laird, G. Landsberg, J. Lee, Z. Mao, M. Narain, J. Pazzini, S. Piperov, S. Sagir[64], R. Syarif, D. Yu

University of California, Davis, Davis, USA

R. Band, C. Brainerd, R. Breedon, D. Burns, M. Calderon De La BarcaSanchez, M. Chertok, J. Conway, R. Conway, P. T. Cox, R. Erbacher, C. Flores, G. Funk, W. Ko, O. Kukral, R. Lander, C. Mclean, M. Mulhearn, D. Pellett, J. Pilot, S. Shalhout, M. Shi, D. Stolp, D. Taylor, K. Tos, M. Tripathi, Z. Wang, F. Zhang

University of California, Los Angeles, USA

M. Bachtis, C. Bravo, R. Cousins, A. Dasgupta, A. Florent, J. Hauser, M. Ignatenko, N. Mccoll, S. Regnard, D. Saltzberg, C. Schnaible, V. Valuev

University of California, Riverside, Riverside, USA

E. Bouvier, K. Burt, R. Clare, J. W. Gary, S. M. A. GhiasiShirazi, G. Hanson, G. Karapostoli, E. Kennedy, F. Lacroix, O. R. Long, M. OlmedoNegrete, M. I. Paneva, W. Si, L. Wang, H. Wei, S. Wimpenny, B. R. Yates

University of California, San Diego, LJ, USA

J. G. Branson, S. Cittolin, M. Derdzinski, R. Gerosa, D. Gilbert, B. Hashemi, A. Holzner, D. Klein, G. Kole, V. Krutelyov, J. Letts, M. Masciovecchio, D. Olivito, S. Padhi, M. Pieri, M. Sani, V. Sharma, S. Simon, M. Tadel, A. Vartak, S. Wasserbaech[65], J. Wood, F. Würthwein, A. Yagil, G. Zevi Della Porta

University of California, Santa Barbara - Department of Physics, Santa Barbara, USA

N. Amin, R. Bhandari, J. Bradmiller-Feld, C. Campagnari, M. Citron, A. Dishaw, V. Dutta, M. FrancoSevilla, L. Gouskos, R. Heller, J. Incandela, A. Ovcharova, H. Qu, J. Richman, D. Stuart, I. Suarez, S. Wang, J. Yoo

California Institute of Technology, Pasadena, USA

D. Anderson, A. Bornheim, J. Bunn, J. M. Lawhorn, H. B. Newman, T. Q. Nguyen, M. Spiropulu, J. R. Vlimant, R. Wilkinson, S. Xie, Z. Zhang, R. Y. Zhu

Carnegie Mellon University, Pittsburgh, USA

M. B. Andrews, T. Ferguson, T. Mudholkar, M. Paulini, M. Sun, I. Vorobiev, M. Weinberg

University of Colorado Boulder, Boulder, USA

J. P. Cumalat, W. T. Ford, F. Jensen, A. Johnson, M. Krohn, S. Leontsinis, E. MacDonald, T. Mulholland, K. Stenson, K. A. Ulmer, S. R. Wagner

Cornell University, Ithaca, USA

J. Alexander, J. Chaves, Y. Cheng, J. Chu, A. Datta, K. Mcdermott, N. Mirman, J. R. Patterson, D. Quach, A. Rinkevicius, A. Ryd, L. Skinnari, L. Soffi, S. M. Tan, Z. Tao, J. Thom, J. Tucker, P. Wittich, M. Zientek

Fermi National Accelerator Laboratory, Batavia, USA

S. Abdullin, M. Albrow, M. Alyari, G. Apollinari, A. Apresyan, A. Apyan, S. Banerjee, L. A. T. Bauerdick, A. Beretvas, J. Berryhill, P. C. Bhat, G. Bolla[†], K. Burkett, J. N. Butler, A. Canepa, G. B. Cerati, H. W. K. Cheung, F. Chlebana, M. Cremonesi, J. Duarte, V. D. Elvira, J. Freeman, Z. Gecse, E. Gottschalk, L. Gray, D. Green, S. Grünendahl, O. Gutsche, J. Hanlon, R. M. Harris, S. Hasegawa, J. Hirschauer, Z. Hu, B. Jayatilaka, S. Jindariani, M. Johnson, U. Joshi, B. Klima, M. J. Kortelainen, B. Kreis, S. Lammel, D. Lincoln, R. Lipton, M. Liu, T. Liu, J. Lykken, K. Maeshima, J. M. Marraffino, D. Mason, P. McBride, P. Merkel, S. Mrenna, S. Nahn, V. O'Dell, K. Pedro, C. Pena, O. Prokofyev, G. Rakness, L. Ristori, A. Savoy-Navarro[66], B. Schneider, E. Sexton-Kennedy, A. Soha, W. J. Spalding, L. Spiegel, S. Stoynev, J. Strait, N. Strobbe, L. Taylor, S. Tkaczyk, N. V. Tran, L. Uplegger, E. W. Vaandering, C. Vernieri, M. Verzocchi, R. Vidal, M. Wang, H. A. Weber, A. Whitbeck

University of Florida, Gainesville, USA

D. Acosta, P. Avery, P. Bortignon, D. Bourilkov, A. Brinkerhoff, A. Carnes, M. Carver, D. Curry, R. D. Field, S. V. Gleyzer, B. M. Joshi, J. Konigsberg, A. Korytov, P. Ma, K. Matchev, H. Mei, G. Mitselmakher, K. Shi, D. Sperka, J. Wang, S. Wang

Florida International University, Miami, USA

Y. R. Joshi, S. Linn

Florida State University, Tallahassee, USA

A. Ackert, T. Adams, A. Askew, S. Hagopian, V. Hagopian, K. F. Johnson, T. Kolberg, G. Martinez, T. Perry, H. Prosper, A. Saha, A. Santra, V. Sharma, R. Yohay

Florida Institute of Technology, Melbourne, USA

M. M. Baarmand, V. Bhopatkar, S. Colafranceschi, M. Hohlmann, D. Noonan, M. Rahmani, T. Roy, F. Yumiceva

University of Illinois at Chicago (UIC), Chicago, USA

M. R. Adams, L. Apanasevich, D. Berry, R. R. Betts, R. Cavanaugh, X. Chen, S. Dittmer, O. Evdokimov, C. E. Gerber, D. A. Hangal, D. J. Hofman, K. Jung, J. Kamin, C. Mills, I. D. Sandoval Gonzalez, M. B. Tonjes, N. Varelas, H. Wang, Z. Wu, J. Zhang

The University of Iowa, Iowa City, USA

M. Alhusseini, B. Bilki[67], W. Clarida, K. Dilsiz[68], S. Durgut, R. P. Gandrajula, M. Haytmyradov, V. Khristenko, J.-P. Merlo, A. Mestvirishvili, A. Moeller, J. Nachtman, H. Ogul[69], Y. Onel, F. Ozok[70], A. Penzo, C. Snyder, E. Tiras, J. Wetzel

Johns Hopkins University, Baltimore, USA

B. Blumenfeld, A. Cocoros, N. Eminizer, D. Fehling, L. Feng, A. V. Gritsan, W. T. Hung, P. Maksimovic, J. Roskes, U. Sarica, M. Swartz, M. Xiao, C. You

The University of Kansas, Lawrence, USA

A. Al-bataineh, P. Baringer, A. Bean, S. Boren, J. Bowen, J. Castle, S. Khalil, A. Kropivnitskaya, D. Majumder, W. Mcbrayer, M. Murray, C. Rogan, S. Sanders, E. Schmitz, J. D. Tapia Takaki, Q. Wang

Kansas State University, Manhattan, USA

A. Ivanov, K. Kaadze, D. Kim, Y. Maravin, D. R. Mendis, T. Mitchell, A. Modak, A. Mohammadi, L. K. Saini, N. Skhirtladze

Lawrence Livermore National Laboratory, Livermore, USA

F. Rebassoo, D. Wright

University of Maryland, College Park, USA

A. Baden, O. Baron, A. Belloni, S. C. Eno, Y. Feng, C. Ferraioli, N. J. Hadley, S. Jabeen, G. Y. Jeng, R. G. Kellogg, J. Kunkle, A. C. Mignerey, F. Ricci-Tam, Y. H. Shin, A. Skuja, S. C. Tonwar, K. Wong

Massachusetts Institute of Technology, Cambridge, USA

D. Abercrombie, B. Allen, V. Azzolini, R. Barbieri, A. Baty, G. Bauer, R. Bi, S. Brandt, W. Busza, I. A. Cali, M. D'Alfonso, Z. Demiragli, G. GomezCeballos, M. Goncharov, P. Harris, D. Hsu, M. Hu, Y. Iiyama, G. M. Innocenti, M. Klute, D. Kovalskyi, Y.-J. Lee, A. Levin, P. D. Luckey, B. Maier, A. C. Marini, C. Mcginn, C. Mironov, S. Narayanan, X. Niu, C. Paus, C. Roland, G. Roland, G. S. F. Stephans, K. Sumorok, K. Tatar, D. Velicanu, J. Wang, T. W. Wang, B. Wyslouch, S. Zhaozhong

University of Minnesota, Minneapolis, USA

A. C. Benvenuti, R. M. Chatterjee, A. Evans, P. Hansen, S. Kalafut, Y. Kubota, Z. Lesko, J. Mans, S. Nourbakhsh, N. Ruckstuhl, R. Rusack, J. Turkewitz, M. A. Wadud

University of Mississippi, Oxford, USA

J. G. Acosta, S. Oliveros

University of Nebraska-Lincoln, Lincoln, USA

E. Avdeeva, K. Bloom, D. R. Claes, C. Fangmeier, F. Golf, R. Gonzalez Suarez, R. Kamalieddin, I. Kravchenko, J. Monroy, J. E. Siado, G. R. Snow, B. Stieger

State University of New York at Buffalo, Buffalo, USA

A. Godshalk, C. Harrington, I. Iashvili, A. Kharchilava, D. Nguyen, A. Parker, S. Rappoccio, B. Roozbahani

Northeastern University, Boston, USA

G. Alverson, E. Barberis, C. Freer, A. Hortiangtham, D. M. Morse, T. Orimoto, R. Teixeira De Lima, T. Wamorkar, B. Wang, A. Wisecarver, D. Wood

Northwestern University, Evanston, USA

S. Bhattacharya, O. Charaf, K. A. Hahn, N. Mucia, N. Odell, M. H. Schmitt, K. Sung, M. Trovato, M. Velasco

University of Notre Dame, Notre Dame, USA

R. Bucci, N. Dev, M. Hildreth, K. Hurtado Anampa, C. Jessop, D. J. Karmgard, N. Kellams, K. Lannon, W. Li, N. Loukas, N. Marinelli, F. Meng, C. Mueller, Y. Musienko[34], M. Planer, A. Reinsvold, R. Ruchti, P. Siddireddy, G. Smith, S. Taroni, M. Wayne, A. Wightman, M. Wolf, A. Woodard

The Ohio State University, Columbus, USA

J. Alimena, L. Antonelli, B. Bylsma, L. S. Durkin, S. Flowers, B. Francis, A. Hart, C. Hill, W. Ji, T. Y. Ling, W. Luo, B. L. Winer, H. W. Wulsin

Princeton University, Princeton, USA

S. Cooperstein, P. Elmer, J. Hardenbrook, P. Hebda, S. Higginbotham, A. Kalogeropoulos, D. Lange, J. Luo, D. Marlow, K. Mei, I. Ojalvo, J. Olsen, C. Palmer, P. Piroué, J. Salfeld-Nebgen, D. Stickland, C. Tully

University of Puerto Rico, Mayagüez, USA

S. Malik, S. Norberg

Purdue University, West Lafayette, USA

A. Barker, V. E. Barnes, S. Das, L. Gutay, M. Jones, A. W. Jung, A. Khatiwada, D. H. Miller, N. Neumeister, C. C. Peng, H. Qiu, J. F. Schulte, J. Sun, F. Wang, R. Xiao, W. Xie

Purdue University Northwest, Hammond, USA

T. Cheng, J. Dolen, N. Parashar

Rice University, Houston, USA

Z. Chen, K. M. Ecklund, S. Freed, F. J. M. Geurts, M. Guilbaud, M. Kilpatrick, W. Li, B. Michlin, B. P. Padley, J. Roberts, J. Rorie, W. Shi, Z. Tu, J. Zabel, A. Zhang

University of Rochester, Rochester, USA

A. Bodek, P. de Barbaro, R. Demina, Y. t. Duh, J. L. Dulemba, C. Fallon, T. Ferbel, M. Galanti, A. Garcia-Bellido, J. Han, O. Hindrichs, A. Khukhunaishvili, K.H. Lo, P. Tan, R. Taus, M. Verzetti

Rutgers, The State University of New Jersey, Piscataway, USA

A. Agapitos, J. P. Chou, Y. Gershtein, T. A. Gómez Espinosa, E. Halkiadakis, M. Heindl, E. Hughes, S. Kaplan, R. KunnawalkamElayavalli, S. Kyriacou, A. Lath, R. Montalvo, K. Nash, M. Osherson, H. Saka, S. Salur, S. Schnetzer, D. Sheffield, S. Somalwar, R. Stone, S. Thomas, P. Thomassen, M. Walker

University of Tennessee, Knoxville, USA

A. G. Delannoy, J. Heideman, G. Riley, K. Rose, S. Spanier, K. Thapa

Texas A&M University, College Station, USA

O. Bouhali[71], A. Castaneda Hernandez[71], A. Celik, M. Dalchenko, M. De Mattia, A. Delgado, S. Dildick, R. Eusebi, J. Gilmore, T. Huang, T. Kamon[72], S. Luo, R. Mueller, Y. Pakhotin, R. Patel, A. Perloff, L. Perniè, D. Rathjens, A. Safonov, A. Tatarinov

Texas Tech University, Lubbock, USA

N. Akchurin, J. Damgov, F. De Guio, P. R. Dudero, S. Kunori, K. Lamichhane, S. W. Lee, T. Mengke, S. Muthumuni, T. Peltola, S. Undleeb, I. Volobouev, Z. Wang

Vanderbilt University, Nashville, USA

S. Greene, A. Gurrola, R. Janjam, W. Johns, C. Maguire, A. Melo, H. Ni, K. Padeken, J. D. Ruiz Alvarez, P. Sheldon, S. Tuo, J. Velkovska, Q. Xu

University of Virginia, Charlottesville, USA

M. W. Arenton, P. Barria, B. Cox, R. Hirosky, M. Joyce, A. Ledovskoy, H. Li, C. Neu, T. Sinthuprasith, Y. Wang, E. Wolfe, F. Xia

Wayne State University, Detroit, USA

R. Harr, P. E. Karchin, N. Poudyal, J. Sturdy, P. Thapa, S. Zaleski

University of Wisconsin-Madison, Madison, WI, USA

M. Brodski, J. Buchanan, C. Caillol, D. Carlsmith, S. Dasu, L. Dodd, S. Duric, B. Gomber, M. Grothe, M. Herndon, A. Hervé, U. Hussain, P. Klabbers, A. Lanaro, A. Levine, K. Long, R. Loveless, T. Ruggles, A. Savin, N. Smith, W. H. Smith, N. Woods

[†] **Deceased**

1: Also at Vienna University of Technology, Vienna, Austria

2: Also at IRFU, CEA, Université Paris-Saclay, Gif-sur-Yvette, France

3: Also at Universidade Estadual de Campinas, Campinas, Brazil

4: Also at Federal University of Rio Grande do Sul, Porto Alegre, Brazil

5: Also at Université Libre de Bruxelles, Brussels, Belgium

6: Also at Institute for Theoretical and Experimental Physics, Moscow, Russia

7: Also at Joint Institute for Nuclear Research, Dubna, Russia

8: Now at Cairo University, Cairo, Egypt

9: Also at Zewail City of Science and Technology, Zewail, Egypt

10: Also at British University in Egypt, Cairo, Egypt

11: Now at Ain University, Cairo, Egypt

12: Also at Department of Physics, King Abdulaziz University, Jeddah, Saudi Arabia

13: Also at Université de Haute Alsace, Mulhouse, France

14: Also at Skobeltsyn Institute of Nuclear Physics, Lomonosov Moscow State University, Moscow, Russia

15: Also at Tbilisi State University, Tbilisi, Georgia

16: Also at CERN, European Organization for Nuclear Research, Geneva, Switzerland

17: Also at RWTH Aachen University, III. Physikalisches Institut A, Aachen, Germany

18: Also at University of Hamburg, Hamburg, Germany

19: Also at Brandenburg University of Technology, Cottbus, Germany

20: Also at Institute of Nuclear Research ATOMKI, Debrecen, Hungary

21: Also at MTA-ELTE Lendület CMS Particle and Nuclear Physics Group, Eötvös Loránd University, Budapest, Hungary

22: Also at Institute of Physics, University of Debrecen, Debrecen, Hungary

23: Also at Indian Institute of Technology Bhubaneswar, Bhubaneswar, India

24: Also at Institute of Physics, Bhubaneswar, India

25: Also at Shoolini University, Solan, India

26: Also at University of Visva-Bharati, Santiniketan, India

27: Also at Isfahan University of Technology, Isfahan, Iran

28: Also at Plasma Physics Research Center, Science and Research Branch, Islamic Azad University, Tehran, Iran

29: Also at Università degli Studi di Siena, Siena, Italy

30: Also at International Islamic University of Malaysia, Kuala Lumpur, Malaysia

31: Also at Malaysian Nuclear Agency, MOSTI, Kajang, Malaysia

32: Also at Consejo Nacional de Ciencia y Tecnología, Mexico city, Mexico

33: Also at Warsaw University of Technology, Institute of Electronic Systems, Warsaw, Poland

34: Also at Institute for Nuclear Research, Moscow, Russia

35: Now at National Research Nuclear University 'Moscow Engineering Physics Institute' (MEPhI), Moscow, Russia

36: Also at St. Petersburg State Polytechnical University, St. Petersburg, Russia

37: Also at University of Florida, Gainesville, USA

38: Also at P.N. Lebedev Physical Institute, Moscow, Russia

39: Also at California Institute of Technology, Pasadena, USA

40: Also at Budker Institute of Nuclear Physics, Novosibirsk, Russia

41: Also at Faculty of Physics, University of Belgrade, Belgrade, Serbia

42: Also at INFN Sezione di Pavia[a], Università di Pavia[b], Pavia, Italy

43: Also at University of Belgrade, Faculty of Physics and Vinca Institute of Nuclear Sciences, Belgrade, Serbia

44: Also at Scuola Normale e Sezione dell'INFN, Pisa, Italy

45: Also at National and Kapodistrian University of Athens, Athens, Greece

46: Also at Riga Technical University, Riga, Latvia

47: Also at Universität Zürich, Zurich, Switzerland

48: Also at Stefan Meyer Institute for Subatomic Physics, (SMI), Vienna, Austria

49: Also at Adiyaman University, Adiyaman, Turkey

50: Also at Istanbul Aydin University, Istanbul, Turkey

51: Also at Mersin University, Mersin, Turkey

52: Also at Piri Reis University, Istanbul, Turkey

53: Also at Gaziosmanpasa University, Tokat, Turkey

54: Also at Ozyegin University, Istanbul, Turkey

55: Also at Izmir Institute of Technology, Izmir, Turkey

56: Also at Marmara University, Istanbul, Turkey

57: Also at Kafkas University, Kars, Turkey

58: Also at Istanbul Bilgi University, Istanbul, Turkey

59: Also at Hacettepe University, Ankara, Turkey

60: Also at Rutherford Appleton Laboratory, Didcot, UK

61: Also at School of Physics and Astronomy, University of Southampton, Southampton, UK

62: Also at Monash University, Faculty of Science, Clayton, Australia

63: Also at Bethel University, St. Paul, USA

64: Also at Karamanoğlu Mehmetbey University, Karaman, Turkey

65: Also at Utah Valley University, Orem, USA

66: Also at Purdue University, West Lafayette, USA

67: Also at USABeykent University, Istanbul, Turkey

68: Also at Bingol University, Bingöl, Turkey

69: Also at Sinop University, Sinop, Turkey

70: Also at Mimar Sinan University, Istanbul, Istanbul, Turkey

71: Also at Texas A&M University at Qatar, Doha, Qatar

72: Also at Kyungpook National University, Daegu, Korea